Helium nanodroplet isolation rovibrational spectroscopy: Methods and recent results

Carlo Callegari, Kevin K. Lehmann,[a] Roman Schmied, and Giacinto Scoles[b]
Department of Chemistry, Princeton University, Princeton, New Jersey 08544

(Received 1 August 2001; accepted 26 September 2001)

In this article, recent developments in helium nanodroplet isolation (HENDI) spectroscopy are reviewed, with an emphasis on the infrared region of the spectrum. We discuss how molecular beam spectroscopy and matrix isolation spectroscopy can be usefully combined into a method that provides a unique tool to tackle physical and chemical problems which had been outside our experimental possibilities. Next, in reviewing the experimental methodology, we present design criteria for droplet beam formation and its seeding with the chromophore(s) of interest, followed by a discussion of the merits and shortcomings of radiation sources currently used in this type of spectroscopy. In a second, more conceptual part of the review, we discuss several HENDI issues which are understood by the community to a varied level of depth and precision. In this context, we show first how a superfluid helium cluster adopts the symmetry of the molecule or complex seeded in it and discuss the nature of the potential well (and its anisotropy) that acts on a solute inside a droplet, and of the energy levels that arise because of this confinement. Second, we treat the question of the homogeneous versus inhomogeneous broadening of the spectral profiles, moving after this to a discussion of the rotational dynamics of the molecules and of the surrounding superfluid medium. The change in rotational constants from their gas phase values, and their dependence on the angular velocity and vibrational quantum number are discussed. Finally, the spectral shifts generated by this very gentle matrix are analyzed and shown to be small because of a cancellation between the opposing action of the attractive and repulsive parts of the potential of interaction between molecules and their solvent. The review concludes with a discussion of three recent applications to (a) the synthesis of far-from-equilibrium molecular aggregates that could hardly be prepared in any other way, (b) the study of the influence of a simple and rather homogeneous solvent on large amplitude molecular motions, and (c) the study of mixed ^{3}He/^{4}He and other highly quantum clusters (e.g., H_2 clusters) prepared inside helium droplets and interrogated by measuring the IR spectra of molecules embedded in them. In spite of the many open questions, we hope to convince the reader that HENDI has a great potential for the solution of several problems in modern chemistry and condensed matter physics, and that, even more interestingly, this unusual environment has the potential to generate new sets of issues which were not in our minds before its introduction.
[DOI: 10.1063/1.1418746]

I. INTRODUCTION

A. Scope of the review

In this article we review the motivations and the experimental methodology of helium nanodroplet isolation (HENDI) spectroscopy, with an emphasis on the infrared region of the spectrum. After reviewing spectrometer design criteria and experimental know-how, we summarize our present understanding of line spacings, line shapes, and spectral shifts, and discuss some of the recent results in as far as they illustrate general principles and possible future applications. Our aim is centered on discussing the current understanding of the field, on identifying unsolved problems and open questions, and not on providing a complete summary of the work published so far, because the last three years have seen a really explosive growth in this area. For earlier reviews of this field, see Refs. 1 and 2. Before describing the motivations and general goals of this kind of research, we shall first show how the natural evolution of supersonic molecular beam infrared spectroscopy has led seamlessly to this apparently esoteric, but in reality simple, extension, which, as we hope to show here, is likely to spawn a large number of scientific and technical applications.

B. The marriage between molecular beams and matrix spectroscopy

Because of the long fluorescence lifetimes of vibrationally excited molecules, it is impractical, with few exceptions,[3,4] to obtain infrared spectra in free jets using fluorescence detection. At the same time, when the use of well collimated beams is called for, direct measurement of the attenuation of the exciting radiation is also out of the question.[5]

[a]Electronic mail: lehmann@princeton.edu
[b]Electronic mail: gscoles@princeton.edu

This leaves bolometric detection of the energy deposited in the beam by a resonant, tunable laser as the method of choice for this type of spectroscopy.[6] Assuming unity partition function and full saturation of the IR transition, it can be shown that with a seeded beam of ''standard'' intensity and the typical sensitivity of a doped Si (or Ge) bolometer operating at 1.5 K (noise equivalent power on the order of 100 $fW/\sqrt{Hz}$), signal-to-noise (S/N) ratios of up to 10^5 can be obtained.[5]

The method is equally applicable to van der Waals complexes which, again with very few exceptions,[7] dissociate upon vibrational excitation. What is detected in this case is a *decrease* of the total kinetic energy carried by the beam, because the dissociation fragments are deflected from the beam axis, resulting in a decreased particle flux to the detector.

If the complex consists of a large number of monomer units, it is not *a priori* obvious that absorption of energy must lead to evaporation, as the amount of excess energy per degree of freedom can conceivably be too small. One must consider, however, that the temperature of large van der Waals clusters is determined by evaporative cooling,[8] which is a self-limiting process. It is then easy to appreciate that the absorption of an IR photon by a large van der Waals cluster will in general put the cluster above the threshold for evaporation to resume.

Using this detection technique and concepts, IR spectra of hundreds of van der Waals complexes (mostly below 4 monomer units) have been obtained during the last 20 years, contributing a great deal to our knowledge of intermolecular forces.[7,9] For larger sizes, many experiments investigate a single chromophore molecule complexed to a cluster of rare gas atoms, in order to keep the interactions as simple as possible. This class of experiments has, however, about an order of magnitude lower S/N ratios than the experiments carried out on a seeded beam of stable molecules.

In spite of the added difficulties, the possibility of loading a large rare-gas host cluster with almost any chromophore by pickup of the latter in a ''scattering'' cell located on the path of the host cluster beam[10] has generated a whole new class of experiments. As the exact number of atoms in the cluster gradually becomes inconsequential, this approach can be seen as the gas-phase analog of matrix isolation (MI) spectroscopy.[11] As in bulk MI spectroscopy, several classes of experiments can be carried out that involve both the unperturbed chromophore and its photodissociation/reaction products.

In comparison with bulk MI spectroscopy, its cluster isolation (CI) analogue has two main advantages and two major disadvantages. The first advantage is due to the finite size of the cluster matrix, which allows control over the degree of chromophore complexation. Uncontrolled aggregation upon annealing plagues MI spectroscopy and sets one of the inevitable limits of this powerful technique. The second advantage is the fact that preparing the chromophore in a surface location is much easier in a cluster than in a matrix. The two disadvantages are (1) the usual transient character of every molecular beam, which makes it necessary to use powerful laser sources to both pump and probe the cluster beam, while the bulk matrix can be both manipulated and probed with relatively low power, broadband light sources, and (2) the fact that the temperature of a cluster is ''internally set'' by evaporative cooling and cannot easily be changed.

Another problem connected with MI spectroscopy is the presence of matrix-induced perturbations, which can be minimized by the use of bulk solid or liquid helium as a medium. This, however, comes with a heavy price: injection of the sample into helium without causing aggregation or condensation onto the walls of the container is extremely difficult because of low solubility, and has been achieved almost exclusively for atoms.[12] It should be noted, however, that high purity parahydrogen has been shown to form stable matrices for molecular dopants with perturbations, as measured by widths of rovibrational transitions, that are comparable to those observed in helium.[13]

The extension of CI spectroscopy to helium clusters, pioneered at Princeton about a decade ago,[14] solves the problem of sample injection. It has grown tremendously in importance since Toennies' group in Göttingen showed that a guest in a host helium nanodroplet can yield a spectrum indicative of free molecular rotation. Almost all the spectra measured to date are consistent with the spectral structure predicted by the symmetry of the isolated molecule (see Sec. III A). In contrast, in a solid matrix (or even in a conventional liquid, if an instantaneous configuration is considered), the total symmetry of the system is the combined symmetry of the molecule and that of the trapping site, usually lower than that of the molecule alone. Furthermore, the matrix-induced spectral shifts in helium are also much smaller than in any other medium, and often much smaller than complexation-induced shifts (see Sec. III E). For the purpose of comparison with *ab initio* calculations, complexes formed in He droplets can then be treated as isolated (gas phase), and the observed shifts provide direct information to decide which isomers are actually formed. There are two important implications: (1) the structural information contained in the spectral symmetry is undiluted, and (2) if a complex is formed in helium, the interactions of its parts with the surrounding medium are too weak to significantly affect its equilibrium structure (zero-point motions and, more dramatically, kinetics, are sometimes affected).

Finally, the possibility of obtaining high resolution spectra in helium droplets at 0.38 K and, using ^{3}He, 0.15 K, allows for the study of superfluidity in nanoscale systems, a frontier subject in condensed matter physics that has the potential to give a substantial contribution to our understanding of highly degenerate many-body systems.[15,16]

II. EXPERIMENTAL METHODS

The history of liquid helium cluster/nanodroplet production and the principal methods used for their study have been reviewed in the preceding article by Northby.[17] Here we will instead discuss the design criteria of a typical droplet source for HENDI spectroscopy, with particular focus on those used in our laboratory. The schematic of a typical experimental apparatus is shown in Fig. 1.

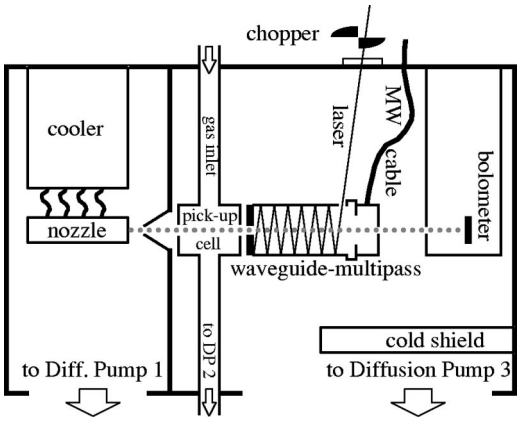

FIG. 1. Schematic of a typical experimental apparatus. From Ref. 18.

A. Nanodroplet beam production

Due to the weak binding energy of small helium clusters, large densities and low temperatures are called for in the expansion, both resulting in a large gas flux. Therefore, liquid helium droplet sources require large pumps and/or very small nozzles. The flux is proportional to $P_0 d^2 T_0^{-1/2}$, where typical nozzle diameters (d) range from 5 to 20 μm, pressures (P_0) from 1 to 100 bar, and temperatures (T_0) from 10 to 30 K. Within the ideal gas approximation, a 10 μm nozzle with $T_0=20$ K and $P_0=15$ bar will discharge into the source chamber approximately the same gas load as a room temperature 50 μm nozzle at 2 bar, i.e., ≈ 4 standard cm^3/s ($=0.16$ mmol/s). This is the maximum gas load that can be applied to a typical diffusion pump with an effective pumping speed of 4000 L/s (referred to N_2, i.e., 10 000 L/s for He) at the limit operating pressure ($\approx 3\times 10^{-4}$ Torr). Typically, droplets with an atom count N of a few thousand are formed. The large mass of these droplets means that the beam intensity is not much affected by scattering from the background gas.

If a source is fed at the ''standard'' load mentioned previously, it is possible to operate a droplet source with a small two-stage closed-cycle refrigerator (the warm stage typically operates at 80 K, the cold stage at 12 K) delivering 1 W of cooling power at the cold stage (0.12 W of power are needed to cool the gas from 80 K down to 20 K). However, due to background radiation and background gas thermal loads, the use of a 5 W refrigerator is recommended. This will allow experiments to span a larger temperature and gas load range, and therefore to cover a larger range of average cluster sizes. For sources which operate below 10 K, which are used for the production of very large clusters ($\langle N\rangle > 10^5$), either refrigerators with lower minimum operating temperatures or direct liquid He cooling are required. Closed-cycle refrigerators with a zero-load temperature of 3 K are commercially available,[19] of course at substantially higher cost. Cost is also the limiting factor for direct liquid He cooling, which is the cooling method that allows the maximum flexibility in terms of droplet size range and total flux that can be attained.[20]

In a subcritical expansion, ^{4}He droplets exhibit a log-normal size distribution, with a full width at half maximum of 0.55–0.75 $\langle N\rangle$.[21,22] While the existence of scaling laws for the determination of $\langle N\rangle$ from expansion parameters is generally recognized, different formulas have been proposed for it.[23] The most popular one states that $\langle N\rangle$ is a function (not necessarily linear)[24] of $P_0 d^{1.5} T_0^{-2.4}$. The estimates that we will give here for $\langle N\rangle$ use a formula by Knuth *et al.*;[25] this formula is in fair agreement with the measurements of Ref. 26, although the latter seem to scale differently with T_0. The case of supercritical expansion, which produces a bimodal distribution of much larger droplets, has been analyzed in Refs. 20, 27, and 28. IR absorption has also been used as a calibrated source of He evaporation to measure average cluster sizes as a function of source conditions.[29]

The exact shape (density distribution) of a He droplet has been computed using both density functional[21,22] and Monte Carlo[30] methods. A good approximation for ''back of the envelope'' calculations is that of a sphere having the same density as bulk liquid helium ($\rho_0=0.0218$ Å^{-3}, for ^{4}He).[31] According to this liquid drop model, a droplet containing N ^{4}He atoms has a radius $R=2.22N^{1/3}$ Å. A more realistic description uses the analytic function:[21,32]

$$\rho(r)=\frac{\rho_0}{2}\left[1-\tanh\left(2\frac{r-R}{g}\right)\right],$$

which accounts for the diffuseness of the surface via a thickness parameter g; the 10%–90% thickness ($\approx 1.1g$) is estimated by various methods to be ≈ 6 Å for ^{4}He (Ref. 21) and ≈ 8 Å for ^{3}He.[22]

The equilibrium temperature of a droplet is dictated by evaporative cooling,[33,34] and can be extracted from the fit of the rovibrational spectrum of a probe molecule (Sec. II D 1). The measured values, 0.38 K for ^{4}He (Ref. 35, and most entries in Table I) and 0.15 K for ^{3}He,[35] are in good agreement with theoretical predictions.[33,34]

About 1 cm downstream from the nozzle, the droplet beam is collimated by a skimmer. As shock waves may play a role in attenuating the beam, it is important that the shape of the skimmer is optimized, and that its edges are as sharp as possible. Typically, commercial electroformed conical skimmers, about 500 μm in diameter, are used.[36]

To give an idea of what intensity can be expected for a droplet beam, consider a detector located 500 mm away from the source, with a 1 mm^2 detection area, and an average cluster size of $\langle N\rangle \approx 4000$. Assuming that 10% of the flux is in the droplets and that the droplet flux is spread uniformly over 1/10 of a steradian in the forward direction (a conservative estimate), one gets a flux of on the order of 10^{11} droplets/s at the detector.[37] Notorious difficulties in calibrating the absolute values of molecular beam detectors (be it bolometers or mass spectrometers) make this number hard to calculate precisely. For larger clusters, a first approximation of the observable mass flux can be obtained by scaling the number of clusters inversely with the number of atoms per cluster.

Whereas pure and doped ^{4}He droplets have been extensively studied far fewer experiments with pure ^{3}He or mixed ^{3}He/^{4}He droplets have been done[15,22,35,38–42] chiefly due to the high cost of the isotope.[43] Budget dictates that ^{3}He be continuously recycled, requiring specialized equipment: sealed pumps and a purification system. The gas is collected

TABLE I. Rotational constants derived from rotationally resolved IR or MW spectra. Blank entries in the "Mode" column indicate purely rotational spectra. The modes in parentheses indicate that more than one band has been seen but the measured rotational constants do not differ enough to grant separate entries.

Molecule	Mode	B_{gas} (cm^{-1})	B_{He} (cm^{-1})	Reference
DCN	⋯	1.208	0.999	77
HCN	⋯	1.478	1.204	77
HCN	ν_1	1.478	1.175	64
$(HCN)_2$	ν_1	0.0582	0.0193	88
$(HCN)_3$	ν_1	0.0156	0.0073	89
HCCCN	ν_1	0.1517	0.0525	18
HCCCN	$2\nu_1$	0.1517	0.0518	69
$(HCCCN)_2$ (*A*)	ν_1 (ν_2)	⋯	0.0168	51
$(HCCCN)_2$ (*B*)	ν_1 (ν_2)	0.0113	0.0050	51
HCCCCH	ν_3	0.1464	0.047	89
$H^{12}C^{12}CH$	ν_3	1.1766	1.0422	49
$H^{13}C^{13}CH$	ν_3	1.1195	0.987	49
CH_3CCH	ν_1	0.2851	0.0741	87
CF_3CCH	$2\nu_1$	0.2851	0.0717	69
CH_3CCH	$2\nu_1$ (*A*)	0.1908	0.1004	69
CF_3CCH	$2\nu_1$ (*B*)	0.0960	0.0355	69
$HCN–N_2$	ν_1	0.0525	0.019	89
HF	ν_1	19.787	19.47	67
$(HF)_2$	ν_1 (ν_2)	0.2167	0.0986	66
CO–HF	ν_1	0.524	0.1022	89
N_2–HF	ν_1	0.1066	0.045	89
$OC^{32}S$	ν_3	0.2029	0.0732	90
$OC^{34}S$	ν_3	0.1979	0.0706	90
$pH_2–OC^{34}S$ (*A*)	ν_3	⋯	0.0847	55
$pH_2–OC^{34}S$ (*B*)	ν_3	⋯	0.0544	55
$pH_2–OC^{34}S$ (*C*)	ν_3	⋯	0.0422	55
SF_6	ν_3	0.0911	0.034	54
HCOOH (*A*)	ν_2 (ν_1)	2.5758	1.3811	91
HCOOH (*B*)	ν_2 (ν_1)	0.4020	0.2970	91
HCOOH (*C*)	ν_2 (ν_1)	0.3470	0.1996	91
DCOOH (*A*)	ν_1	⋯	1.16	91
DCOOH (*B*)	ν_1	⋯	0.24	91
DCOOH (*C*)	ν_1	⋯	0.21	91
CO_2	ν_3	0.39	0.154	92
NH_3	ν_2	9.96	7.5	61
oH_2–HF	ν_1	0.8325	0.182	89
pD_2–HF	ν_1	0.492	0.164	89
oD_2–HF	ν_1	0.487	0.159	89
CH_4	ν_3	5.2406	5.013	150
N_2O	$\nu_1+\nu_3$	0.419	0.0717	92
$(CH_3)_3SiCCH$ (*A*)	$2\nu_1$	0.1056	0.0275	69
$(CH_3)_3SiCCH$ (*B*)	$2\nu_1$	0.0654	0.0144	69
Ar–HF	ν_1	0.102	0.04	89
Cyclopropane ($A+B$)	ν_8	0.6702	0.1631	89
Cyclopropane (*C*)	ν_8	0.4188	0.2416	89
oH_2–HCN	ν_1	0.4303	0.0893	151
pD_2–HCN	ν_1	0.2663	0.0805	151
Mg–HCN	ν_1	⋯	0.0285	68
Mg_3–HCN (*A*)	ν_1	⋯	0.035	68
Mg_3–HCN (*B*)	ν_1	⋯	0.0167	68

from the exhaust of the source chamber pumping system, cleaned on liquid-nitrogen-cooled zeolite traps, pressurized by a membrane compressor to 20–80 bar and fed back to the nozzle. The recycling system used in Refs. 22, 35, and 40–42 needed about 20 bar *l* gas to be filled. The loss rate under normal operation was <2 bar *l* per week.[42] Thus although a considerable initial investment is required the operating costs are comparable to the other running costs of these experiments.

There is an important difference between ^4He_N and ^3He_N clusters: whereas the former are bound for any N,[44] calculations predict that small ^{3}He droplets of less than about 30 atoms are unstable[45,46] because of the larger zero point energy associated with the lighter isotopic mass. Experimentally, a strikingly different behavior of average droplet size as a function of nozzle temperature is observed for the two isotopes. Whereas the size of ^{4}He droplets increases gradually with decreasing temperature,[21] the formation of ^{3}He droplets sets in sharply, and at a considerably lower temperature ($T_0=11.5$ K for $P_0=20$ bar and $d=5\,\mu$m, giving droplets of about 4500 atoms).[22,42] In the expansion of an isotopic mixture, formation of ^{4}He-enriched mixed droplets is observed.[35,42] The ^{4}He concentration in the droplets is several times higher than that of the expanding mixture ($<4\%$) and depends on the expansion conditions.[42] Because ^{4}He will selectively solvate most dopants, the production of pure ^{3}He droplets requires gas of high isotopic purity ($^4He < 10^{-6}$), which is commercially available.[43]

B. Nanodroplet beam doping

After collimation, the droplets are seeded with the molecule of interest by passing them through a small gas pickup cell where the pressure is tailored to obtain the desired mean number of dopants per droplet. The internal and kinetic energy of the dopant, as well as the energy of solvation, are dissipated into the droplet and result in evaporation of He atoms (200–250 atoms, each taking off 5.5–7 K of energy,[47] are estimated for the pickup of a small molecule such as HCN), leading to a microcanonical system cooled to 0.38 K (we assume pure ^{4}He droplets here). On average, the impact parameter of the molecule is significant (2/3 of the droplet radius), resulting in a mean angular momentum of $\approx 45N^{1/3}\hbar$ per collision with HCN. Likewise, He evaporating at 0.38 K will carry away $10–15\hbar$ of angular momentum per atom. At present, it is not clear how much angular momentum remains in the cluster after evaporative cooling, nor in which form it is stored if it exceeds the thermal values.

A quick estimate of the optimum pickup conditions can be made by assuming unity sticking coefficient and a droplet cross section of $15.5N^{2/3}$ Å^2 (see Sec. II A); further, the droplet's size reduction upon pickup and the nonzero velocity of the gas molecules are neglected (if the latter is accounted for, the collision rate will increase by a factor of $\approx\sqrt{1+(v_m/v_d)^2}$, where $v_d\approx 400$ m/s is the droplet velocity and v_m is the rms velocity of the molecules in the pickup cell). With these approximations (further corrections are discussed in Ref. 48), the pickup process results in a Poisson distribution of the number of dopant molecules per droplet, and a column density corresponding to $\approx 2.5N^{-2/3}$ Pa cm is required to maximize the probability of single pickup. Under typical conditions, the vapor pressure needed for efficient doping of helium droplets is on the order of 10^{-2} Pa, some four orders of magnitude lower than what is typically used in supersonic jet coexpansions. This implies that many species can be doped into helium that are not practical to study by jet

spectroscopy because of the high temperatures involved, which are either difficult to reach or cause thermal decomposition of the species. The large cross sections for the droplets imply that the requirements on vacuum are more stringent than for beam experiments on monomers or small clusters.

Molecules captured by the same droplet are expected to find each other and form van der Waals complexes, but once past the pickup region, each droplet becomes an isolated system and no further aggregation occurs. At the temperature of the droplet, 0.38 K, the rovibrational spectrum of a typical molecule spans ~ 1 cm^{-1}, which is generally smaller than the shifts induced by complexation. Hence, spectra of different small oligomers will not overlap, and pickup of more than one molecule per droplet will only decrease the intensity of the single-molecule spectrum, without affecting its shape. For this reason, at least when one is concerned with monomers and dimers only, high purity of the dopant gas is desirable but not essential. An extreme case is the spectrum of $H^{12}C^{13}CH$, which has been observed[49] at its naturally occurring abundance (2.2%) interleaved to that of $H^{12}C^{12}CH$. The situation is different for higher oligomers, because complexation shifts tend toward an asymptotic limit,[50,51] and the spectra tend to merge. Nevertheless, in a favorable case complexes of OCS with up to 17 hydrogen molecules have been made and spectroscopically resolved,[52] though this was done in mixed $^3He/^4He$ droplets which cool to 0.15 K. Pendular spectroscopy (see Sec. II D 4 and Ref. 50) allows even the modest width of the rotational contours to be collapsed, which is particularly favorable in separating closely spaced oligomer or isomer bands.

C. Radiation sources

Since spectroscopy of doped helium droplets is still a relatively new field, it is often the availability of a suitable radiation source that dictates the choice of the system to be studied. In the early days,[14,53] SF_6 (ν_3 mode) was chosen as a dopant molecule because of its large absorption cross section in a spectral region where watts of radiation (from line-tunable CO_2 lasers) were available.

To achieve rotational resolution, this transition was later studied with a continuously tunable semiconductor (lead salt) laser.[54] The same type of laser was also employed for the beautiful studies of OCS in mixed $^3He/^4He$ carried out in Göttingen.[15,52,55,56]

Pulsed lasers have also been used in early experiments on HF-, H_2O-, or NH_3-doped helium droplets.[57–59] They offer the advantage of high power and wide-range tunability; those come at the price of usually broadband emission, so that it becomes difficult to establish whether the width of the observed spectral lines is determined by the surrounding helium environment or rather by the laser itself (via instrumental linewidth or power broadening).

High power line-tunable gas lasers, cw or pulsed, are still being used up to the present time.[60–63] Because of the sparse set of available lasing frequencies, they are most suited to the investigation of small molecules, with small moments of inertia and therefore well spaced lines. Thanks to their large output power, they have been successfully used to perform saturation measurements.[63]

Most of the experimental spectra to date have been acquired with color center lasers, in the 3 μm region,[18,50,51,64–68] and, to a lesser extent, in the 1.5 μm region.[69] These lasers offer broader tunability range, comparatively large output power (30 and 250 mW, respectively) and high resolution, as they can be stabilized to better than 1 MHz without too much difficulty. Since the 1.5 μm region is used in telecommunications, commercial optical components (e.g., fibers, connectors, and high finesse cavities) are available for this type of measurement.

At these power levels it is possible to bring near saturation a 10 MHz homogeneously broad, strong fundamental transition near 3 μm. If the lines are broader or the transition weaker (as in the case of overtones at 1.5 μm), laser field enhancement devices can be usefully employed (see Sec. II D). Looking at the future, since HENDI spectral lines are rarely narrower than 0.01 cm^{-1} (see Sec. III C) and since pulsed lasers with similar bandwidth are available, it would probably be useful to explore the possibility of developing pulsed helium nanodroplet sources. Pulsed devices that produce small He clusters are already available at present.[70]

For cw beam sources, narrow bandwidth high repetition rate pulsed lasers have recently become available at power levels that allow frequency multiplication and mixing. As the use of regenerative amplifiers has allowed repetition rates up to 10 kHz, the problem of the low duty cycle characteristic of traditional pulsed laser sources can be overcome. For strictly cw laser sources, recent developments that will likely find HENDI applications are cw OPOs[71] and quantum cascade lasers.[72] Quantum cascade lasers offer the advantage of being available to wavelengths as high as ≈ 24 μm,[73] which is going to be particularly useful for the study of large molecules where, at higher frequencies, intramolecular vibrational redistribution (IVR) is an unavoidable source of line broadening and of loss of information.

D. Excitation schemes

1. Infrared

Infrared (IR) spectroscopy in He droplets derives its uniqueness from the fact that the medium still allows rotational resolution (a representative spectrum is shown in Fig. 2), even for relatively large molecules and complexes. This is to be compared to ''classical'' solvents, for which rotational resolution is, at best, only possible for molecules of the smallest moments of inertia. Rotational resolution allows the measurement of the cluster temperature, a very sought after quantity as the following statement (made in 1994) proves:

> But so far no ''thermometer'' to measure a cluster's temperature is available. Worse, there does not even exist a suggestion how to construct one [Ref. 74, Chapter 1.5: *Experiments not possible today*].

Ironically, in the same book, the first results on infrared spectroscopy in He clusters were summarized, and the following prediction was made:

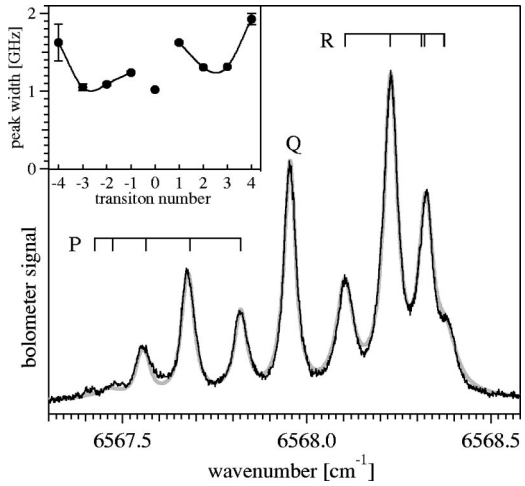

FIG. 2. Spectrum of the $2\nu_1$ transition of propyne, and fit to a symmetric top. The inset shows the linewidth for each transition. Note that at the temperature of the droplet (0.38 K) the Q branch would be absent if nuclear spin relaxation had taken place. From Ref. 69.

> In future the technique may be combined with continuously tunable narrow band lasers of higher power as these become available [*ibid.*, Chapter 3.7: *Infrared spectroscopy*].

Continuously tunable, narrow-band lasers were indeed the key that, one year after, allowed for rotational resolution to be achieved and thus temperature to be measured.[35,54,75] The technical solution that was used to overcome the power requirement consists of a different arrangement of how the laser beam interacts with the beam of doped droplets. In contrast to the opaque bolometer detectors of the early experiments, the use of a ''transparent'' mass spectrometer detector allowed for a setup where the laser and cluster beam counterpropagated, resulting in an interaction region of tens of centimeters. With this arrangement, low power diode lasers can be profitably employed.[54] Additional benefits of using this setup for pulsed lasers is that their duty cycle (defined as the fraction of the beam that is in the laser field) is increased from 10^{-5} to 10^{-3} and the detector output can be time gated to match the depletion transient.

When bolometers are used as detectors, multipass cells[50] and power buildup cavities[69] have been successfully employed. While a well aligned multipass cell can give a 30- to 50-fold increase in signal relative to the single-crossing case, a resonant cavity can further enhance the radiation intensity seen by the droplets by one order of magnitude. Naturally, this comes at a price, since, as the laser is scanned, the cavity has to be kept in resonance by suitable feedback electronics. Moreover, as currently implemented, the interior of the cavity is a volume bound by metallic surfaces; as such it is effectively shielded from electromagnetic fields. Hence, double resonance and Stark spectroscopy experiments are not possible. Nevertheless, the large amount of available power (currently only matched by line-tunable gas lasers)[63] makes this approach very desirable to reach saturation conditions, and to study forbidden transitions.[69]

HENDI spectra have been measured by beam depletion using both bolometers and mass spectrometers to detect the on axis beam flux. Even with helium evaporation occurring at 0.38 K, the mean lab frame scattering angle of the evaporated helium is still $\approx 10°$, and so the evaporated helium atoms largely miss the detector. The relative sensitivity of the two detection methods is hard to determine unambiguously from the literature spectra, as they involve widely different source powers, transition moments, and detection geometries. Our attempt to correct for these factors suggests that detection of depletion with a bolometer is about a factor of 10 more sensitive than with a mass spectrometer. This assumes use of a continuous wave laser and of a multipass cell. The latter partially offsets the shorter excitation length (relative to the more efficient counterpropagation scheme possible with the mass spectrometer) so that ultimately only modest reduction results. The mass spectrometer will likely give superior sensitivity in the case when one is using a low repetition rate pulsed laser for excitation, due to the possibility of using gated detection.

2. Microwaves

Investigation of purely rotational transitions in doped helium clusters shifts the frequency spectrum to the microwave (MW) region. Radiation is confined inside a section of waveguide (part of which is collinear with the cluster beam) properly terminated at the ends. Confinement is necessary not only to concentrate the available microwave power, but also to minimize its absorption or rectification by the bolometric detector, which can easily obscure the true signal.

Pure rotational spectroscopy in He droplets differs from vibrational and electronic spectroscopies in that it is inherently multiphoton. One can see from Table I that in a He droplet the energies associated with a pure rotational transition (0.5–70 GHz) are insufficient to evaporate even a single He atom. Microwave spectroscopy in a He droplet relies on the occurrence of rotational relaxation in an isolated droplet, which allows a dopant molecule to repeatedly absorb photons and release their energy into the droplet. The fact that the observed signals are of the same magnitude as for infrared transitions has been used to estimate the number of relaxation cycles that each molecule must undergo in the ≈ 100 μs it spends in the MW field, and thus to place the rotational relaxation time (see Sec. III C) on the submicrosecond time scale for HCCCN.[76]

The large amount of available microwave power (tens of watts), along with the large transition dipoles in this spectral region has made saturation measurements possible,[18,76,77] which have been used to establish and quantify the dominance of inhomogeneous broadening in HENDI spectroscopy.

3. Double resonance

The term double resonance (DR) refers to the coupling of two transitions by a common level, which allows driving one transition (the ''pump'') to change the strength of the other (the ''probe''). In the gas phase, DR is routinely used (1) to simplify the assignment of complex spectra, (2) to reach states inaccessible by one-photon selection rules, and (3) to measure homogeneous lines within an inhomogeneous

profile. To date, with one exception, only type (3) experiments have been done in helium droplets, and only in the simplest ''steady state'' versions, i.e., without explicit time resolution of the time delay between pump and probe fields. The exception is the recent hole-burning study of the electronic spectrum of tetracene,[78] which shows a helium induced splitting of the electronic band origin. The complexity of the dynamics in helium droplets has unfortunately made the interpretation of these experiments much more difficult than that of their gas phase analogues.

The first double resonance study in helium were the MW–MW experiments performed on the R(3) and R(4) transitions of HCCCN.[76] Saturation measurements on these rotational lines had shown the pattern of a typical line to be dominated by inhomogeneous broadening. It was expected that DR spectra would directly reveal the homogeneous component of the line, as in a classical hole-burning experiment (Ref. 79, page 438). The observation of lines much broader than expected was interpreted as a sign of spectral diffusion (see Sec. III C 2).

In an attempt to gain further insight, MW–IR experiments on HCCCN[18] have been performed. Independent of this work, MW–IR double resonance experiments were performed on OCS.[80] Because rotational relaxation times in He clusters lie in the nanosecond range (during which a cluster only travels a few μm), double resonance experiments require spatial overlap of the two radiation fields. While in MW–MW experiments this is readily achieved, in MW–IR experiments spatial overlap has been achieved by either propagating the laser along the axis of the waveguide,[80] or by using the walls of the waveguide as a substrate for thin mirrors in a multipass arrangement[18] (see Fig. 1). The long wavelength of microwaves, compared to the transverse dimensions of the cluster beam, makes it possible to have holes drilled into the waveguide as ports for the cluster and laser beam, without introducing significant microwave losses.

While a MW–IR scheme introduces the additional complication of vibrational excitation (which fans out the ''probe'' transition frequencies associated with a given ''pump'' frequency), it has the advantage that the probe laser can cover the entire manifold of rotational levels, thus probing rotational states that are not directly connected via the pump field. With some differences, probably due to the use of different molecules, both experiments find that the population of *all* levels is to some extent affected by the pump beam, which indicates fast rotational diffusion.

4. Stark spectroscopy

Stark spectroscopy has been shown to be a potentially valuable tool to learn more about the interactions of the dopant molecule with the helium environment and possible distortions of the molecule (particularly of complexes) by gentle helium solvation.[50,64] In a simple linear dielectric approach, one would expect the molecular dipole moments to be reduced in helium by its dielectric constant, 1.055.[81] However, this is only valid for a dipole in a continuous medium. If the dipole is located in the center of a spherical cavity, the induced dipoles in the solvent cancel out and give no net change in dipole moment. As the solvation around molecules is in general highly anisotropic, the net induced moment provides a potentially interesting measure of the anisotropy. Recently such calculations have been performed for Mg (3P) solvated in He, with the anisotropic density obtained by a density functional method, and a 6.2% reduction of the optical transition dipole of Mg ($3P \rightarrow 3S$) transition has been calculated.[82] Such a reduction, along with the solvent-induced redshift, has been found to quantitatively account for the experimentally measured increased lifetime of the transition. The solvent-induced stabilization of dipolar structures was listed as one of the possible causes of the decreased tunneling splitting observed for the HF dimer in He droplets (see Sec. IV B).

Nauta and Miller[64] have studied the Stark pattern of the R(0) line of HCN in the IR. They find the splitting and intensity pattern expected from the isolated molecule, but with the observation that what appears to be a splitting of the $|M|=0,1$ components persists even at zero field, as a poorly resolved doublet structure of the R(0) line (see Fig. 5). A careful study of the dipole moment in this and other systems would likely be quite valuable for testing theoretical predictions of the helium solvation structure.

Another relevant manifestation of Stark effects is the mixing of rotational states (Ref. 83, Sec. 10.6). In He droplets, it has been exploited to induce a (normally forbidden) Q branch in those linear molecules, such as HCN and HF, whose zero-field rotational constants are large enough that their spectrum consists of the R(0) line only. By this method, the band origin and the rotational constant of the molecule can be directly measured.[64] In this application the field is kept as weak as possible, compatibly with the need of inducing a measurable signal, and indeed an accurate value for the band center is obtained by measuring the position of the Q branch at increasingly weak fields and extrapolating to zero field.

The electric field can be used to ''tune'' the frequency of a given transition. This has been exploited to quench tunneling in $(HF)_2$,[66] and to perform time-resolved relaxation measurements in the ms range (by mapping different excitation times onto an electric field gradient).[84]

Once the information contained in the rovibrational Hamiltonian has been extracted, rotational resolution actually becomes a nuisance: first, the band strength is fractionated, resulting in smaller signals; second, a typical spectrum spans a range comparable to k_BT (0.38 K or 0.26 cm^{-1}), which results in a corresponding loss of resolution when trying to identify closely spaced bands (a common occurrence when many different van der Waals complexes of the same molecules are present). For gas phase polar molecules, an elegant solution is pendular state spectroscopy,[85,86] which is the application of a static electric field sufficiently strong to convert the rotation of a molecule into oscillations of the dipole moment around the external field. In the strong static field limit (and with the permanent and transition moments parallel to each other), the entire rotational contour of the spectrum collapses into a single line at the wave number of the purely vibrational excitation, with an integrated intensity three times that of the entire band at zero field (the traditional spectroscopic ''conservation of intensity'' holds, it is just the

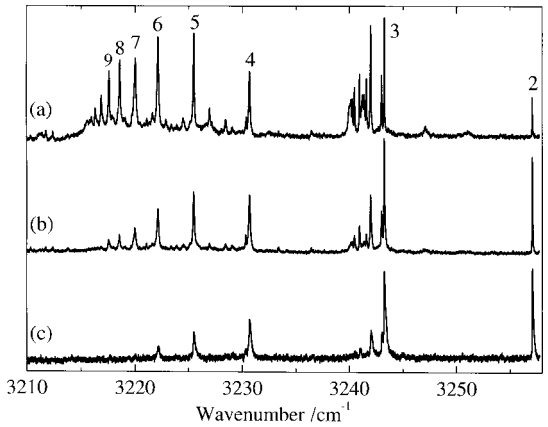

FIG. 3. Stark spectrum of linear chains of cyanoacetylene (labeled by the number of monomer units), showing the high resolution achievable with pendular state spectroscopy. The series is taken at progressively smaller droplet sizes, showing that the size of the droplet limits the length of the chains that can be formed. From Ref. 51, reproduced by permission of The Royal Society of Chemistry.

orientation of the molecules is now fixed, and absorption, no longer averaged, will be maximum when the transition dipole and the laser polarization are parallel). It is indeed possible to use the signal strength as a function of relative polarization of the optical and Stark fields to determine the angle between the static and transition dipoles.

This technique has been applied to He droplets by Nauta and Miller.[50,87] It is particularly attractive in this environment because both the low temperature and the increased moments of inertia make it easier to reach the required ''high field'' limit. By this technique, the spectra of linear chains of up to 8 HCN units,[50] and up to 12 HCCCN units[51] have been resolved (see Sec. IV A and Fig. 3).

Suppression of rotation can also be achieved by replacing ^{4}He with ^{3}He.[15,55] The technique has been used to collapse the absorption bands of OCS–$(H_2)_n$ complexes so that n could be assigned via the measured band shift.[52,56] This method is applicable even to nonpolar cases, but lines will typically not be as narrow as for ^{4}He spectra.

III. CURRENT UNDERSTANDING AND OPEN QUESTIONS

A. Molecular symmetries in the nanodroplet environment

The most remarkable feature of the vibration–rotation spectra of molecules in liquid ^{4}He nanodroplets is the presence of rotational fine structure, either quantum state resolved or observed as rotational contours. This was first seen in the seminal work of Hartmann *et al.*[54] on the spectrum of SF_6, but has now been observed in a wide range of other molecular solutes. Table I contains a list of molecules studied to date with rotational resolution in the IR, at least as known to us. In almost every case, the nature of the spectroscopic rovibrational structure is exactly what one expects from the gas phase, i.e., the standard spectroscopic signatures of a linear, symmetric, or spherical top are preserved, along with the rotational selection rules based upon the symmetry of the gas phase transition dipole moment, though often with dramatically changed spectroscopic constants (see Sec. III D and Fig. 2). High temperature spin statistical weights have been observed, indicative of negligible relaxation between nuclear spin isomers on the time scale of the experiment ($\sim$100 μs), as first noted by Harms *et al.*[35] (see also Fig. 2).

Viewed in terms of a classical picture of the instantaneous configurations of the helium atoms, the above-mentioned preservation of symmetry is unexpected in that these instantaneous configurations do not retain the molecular symmetry. In view of the large delocalization of the He atoms, we must rather consider the symmetry of their ground state many-body wave function, which is the same as the molecular symmetry. Bulk excitations of the helium droplet would lower this symmetry, but at the temperature of the droplets, liquid-drop-model calculations indicate that there are no thermally excited phonons.[34] Thermal excitations are present in the surface modes of the droplet, but these appear to couple weakly to the solvated molecules, though they must ultimately be responsible for the relaxation of the latter into thermal equilibrium with the droplet. Thus, we are lead to view the helium not as a classical fluid of rapidly moving particles, but as a quantum probability density associated with a bosonic N-body wave function, which is a smooth and continuous function of coordinates and reflects the symmetry of the potential that the molecule creates for the helium.

One potential counterargument of the above-mentioned model is that linear molecules will create a cylindrically symmetric ring of helium density around them, implying that the entire system should act as a symmetric top, which has an additional rotational degree of freedom. However, it is easily shown that the Bose symmetry of the helium eliminates the low lying K excited states:[90] states with angular momentum along the symmetry axis cannot be thermally populated, and the $K=0$ spectrum of a symmetric top is indistinguishable from that of a Σ state of a linear molecule (see also Sec. IV D). This argument alone does not exclude the possibility of creating $K>0$ states with modest energy ($\sim$3.2 K has been estimated for OCS in He).[90] However, in order to create such a ''vortex'' excitation localized in the first solvation shell, it is necessary to have a nodal surface separating it from the vortex-free remainder of the helium droplet;[148] such a nodal surface may come at a steep energy cost, making the creation of high-K modes even more difficult. It would be interesting to have an estimate for the excitation energy of such states calculated with the fixed node diffusion Monte Carlo (DMC) method.

Miller's group has observed two examples of spectra of highly polar linear molecules (cyanoacetylene dimer and HCN trimer)[51] which appear to have Q branches, and thus suggest a breakdown of this ''rule'' of preservation of molecular symmetry. The origin of the Q branches in these cases has not yet been explained conclusively. It has been proposed that they arise not from population of higher K states of the helium, but are due to some mechanism that would create an anisotropic potential for rotation of the molecules. One candidate is the anisotropy due to the finite size of the droplet and the delocalization of the molecule in the droplet[51] (see Sec. III B). This model predicted the wrong droplet size dependence of the Q-branch intensity unless an

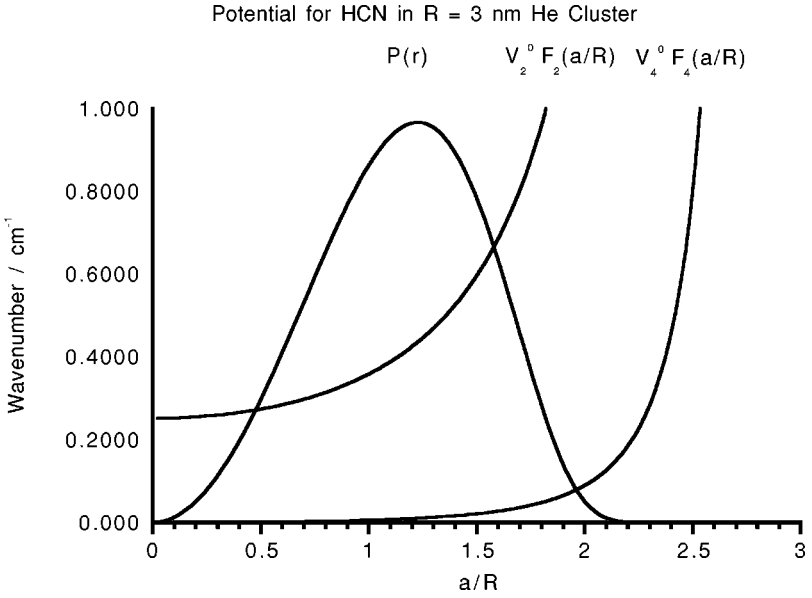

FIG. 4. Isotropic (V_2) and anisotropic (V_4) parts of the confining potential for a dopant molecule (HCN) in He droplets, arising from the dopant–He long-range interaction. $P(r)$ is the radial probability density function for the position of the dopant. From Ref. 95.

ad hoc energy term was added to favor location of the molecule slightly below the helium surface. Another proposal[93] is the presence of a vortex in a minority of droplets, which is expected to strongly align molecules along it.[94] This would also appear to favor Q-branch intensity in smaller droplets since a larger fraction of pickup collisions in such droplets would be expected to impart enough angular momentum to create a vortex (on the order of one $\hbar$ per helium atom). We would like to add to the list the anisotropy that arises from the hydrodynamic coupling of rotation and translation[95] (see Sec. III B), which is expected to be most important for precisely the extremely prolate molecules for which this interesting effect has been observed. Furthermore, this effect should be most important for large droplets, where the motional averaging of the linear momentum (to which the angular momentum is coupled) is slowest. Clearly, these ''odd'' spectra should be subjected to further experimental and theoretical work since some important new dynamical effect may be revealing itself by these phenomena.

It is worth noting that none of the rovibrational spectra observed in helium have shown evidence of ''phonon wings.'' Such features, which appear to the blue of the molecular excitation and involve creation of one or more helium phonons upon solute excitation, are observed and often predominate in electronic spectra.[96,97] The strength of the pure molecular excitation, the zero phonon line (ZPL), is expected to decrease exponentially with the degree of solvent reorganization upon molecular excitation, and thus the complete dominance of the ZPL in the case of vibrational excitation implies that the reorganization of the solvation density must be negligible relative to the zero point fluctuations of the helium ground state density. Perhaps the study of floppy, large amplitude vibrational modes (see Sec. IV B) will show evidence of the phonon wings, which could provide valuable data on solvent reorganization in a quantum liquid.

B. Translational motion of molecules: Where are the molecules?

The gas-phase-like symmetry of rovibrational spectra of molecules attached to helium droplets strongly suggests that these molecules are located in a nearly isotropic environment. This rules out surface sites since their reduced symmetry would lead to a characteristic splitting of the M degeneracy, as has been seen for the electronic spectrum of He_2^* which resides above the surface of the helium.[98] Once a molecule penetrates the helium surface by more than the first or perhaps second solvation layer, a relatively flat potential is expected. Toennies and Vilesov[99] proposed treating the motion of the solvated molecule as that of a free particle in a spherical box. However, one can explicitly calculate the effective potential that pulls the molecule toward the center of the droplet by summing up the missing long-range interactions outside of the droplet (i.e., taking the molecule in bulk helium as the reference state). The resulting potential turns out to localize molecules well within the droplets (see Fig. 4), keeping them away from the surface region where the approximations used to derive the potential are expected to break down.[95] The spectrum of thermally populated energy levels of a particle in this potential resembles more closely that of a three-dimensional harmonic oscillator than that of a particle in a box; the heat capacity arising from this motion is nearly $3k_B$ and is similar to that of an entire, pure helium nanodroplet of 3 nm radius. The effective frequency for vibrational motion in this potential is $\approx 0.5-1$ GHz in typical cases. The potential is proportional to the molecule–helium C_6 coefficient minus the helium–helium C_6 coefficient times the net number of helium atoms displaced by the molecule, i.e., there is a buoyancy correction due to the change in the net helium–helium interaction as the molecule is displaced.[100]

For a non-spherically-symmetric molecule, displacement from the center of the droplet leads to a reduction in site symmetry and a weak coupling between translational and rotational motion. The leading coupling term has a $P_2(\cos\theta)$ dependence on the angle θ between the axis of a linear rotor molecule and the displacement vector from the center of the droplet (P_n are the Legendre polynomials). If the displacements from the center are assumed to be static and their distribution given by Boltzmann weights, this P_2 asymmetric

field results in the same type of characteristic splitting of M components of a transition as discussed previously for a surface location, and is easily calculated analytically. However, calculations indicate that the expected splittings are on the order of, or less than, the vibrational frequency in the 3D potential, and thus the splittings are predicted to be at least partially motionally averaged. Lehmann[95] has given explicit matrix elements for calculations in a coupled basis of translational and rotational angular momenta of the molecule, and presented some sample calculations.

Another important coupling of translational motion and molecular rotation is expected to arise from hydrodynamic effects (see Sec. III D 1). The translational motion of an ellipsoid in helium leads to a hydrodynamic contribution to the effective mass, which depends upon the orientation of the ellipsoid relative to the linear momentum. Lehmann[95] has derived the quantum Hamiltonian including this coupling term, and the resulting matrix elements between the translational and rotational angular momenta. Model calculations on simple systems, such as HCN and OCS, suggest that the hydrodynamic coupling is more important than the potential terms mentioned in the previous paragraph. It is interesting to note that the hydrodynamic term leads again to the expected $P_2(\cos\theta)$ induced splittings in the limit of bulk helium, where the potential asymmetry goes to zero.

The relatively dense manifold of center-of-mass states, coupled to the rotation of the molecule which changes upon rovibrational excitation, creates a source of inhomogeneous broadening in the spectrum that was originally not recognized: quantization of the translational motion should lead to a potentially resolvable fine structure of the spectral features. However, it is likely that the broad droplet size distribution present in all rovibrational spectra observed to date will wash out any details of this fine structure, which is then only observable as a source of inhomogeneous broadening in the spectrum.

These couplings of the center of mass and rotational motion of the molecules are believed to make important contributions to the inhomogeneous line shapes often observed in rovibrational spectra. However, calculations done to date have neglected the vibrational dependence of the interaction of the helium with the molecules. Any such model predicts that the line shape will be independent of vibrational transition, and that the R(J) and P($J-1$) transitions should be mirror images, which is not what is generally observed. Once vibrationally averaged potentials for different vibrational states become available, it will be possible to more critically test the line shapes predicted by this model. At present, it must be admitted we do not have a quantitatively successful theory.

C. Line shapes of rotationally resolved lines

Direct evidence of inhomogeneous broadening is only available for a few molecules; nevertheless, there are reasons to believe that it is common to all molecules. One reason is that the rovibrational lines rarely fit to the Lorentzian shapes predicted by simple lifetime broadening models. This is particularly evident for HCN, for which the R(0) ($J=0\rightarrow1$) transition has been studied in several vibrational states, as well as in the deuterated molecule (see Fig. 5). For OCS, the lines in the P and R branches have tails that point toward the band origin and widths that grow with J. Possible explanations have been discussed by Grebenev *et al.*[90] Available evidence suggests that one can expect inhomogeneous broadening to contribute a few hundred MHz or more to the linewidth, equivalent to a lifetime of a few ns. Often, rotational and vibrational relaxation is slower than that, yet (with the notable exception of vibrationally excited HF)[67] still much faster than the 0.1–1 ms time scale of the experiment.

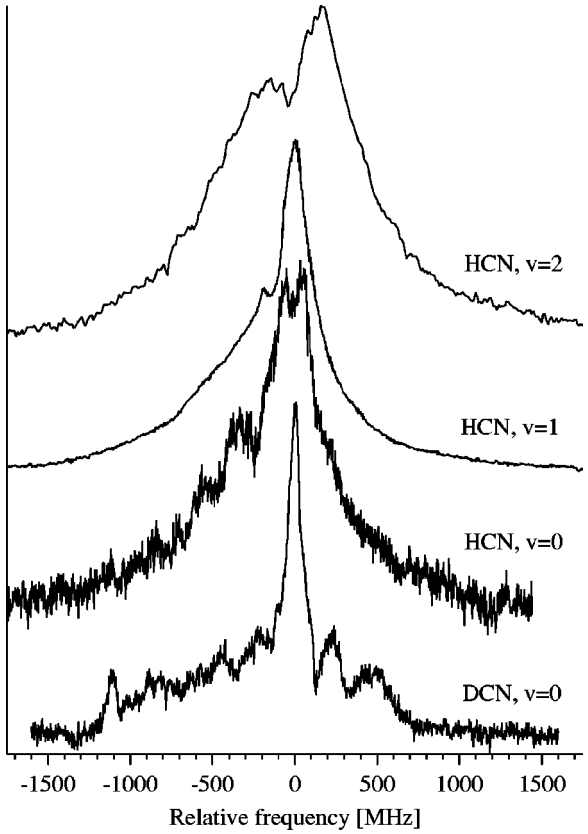

FIG. 5. R(0) line for DCN ($\nu_1=0$) and HCN ($\nu_1=0,1,2$), evidencing the importance of inhomogeneous broadening. These data show that vibrational excitation is not very important in determining the broadening pattern, whereas the mass of the dopant is, suggesting a nontrivial dynamics inside the droplet. The data are adapted from Refs. 77, 77, 64, and 69, respectively. The zero of the frequency was selected to best overlap the transitions.

This slow relaxation derives from the large mismatch between the frequencies of the modes of the molecule and those of the helium bath (the helium cannot respond on the time scale of the vibrational motion of the molecule). The maximum energy of an elementary excitation in bulk ^{4}He is about 20 K.[101] As a result, V–T (vibration to translation) and even most V–V (vibration to vibration) relaxations require simultaneous creation of many (10–100) phonons/rotons in the helium. One expects the rate of such processes to be slow, decreasing exponentially with the number of phonons involved.

1. Homogeneously broadened profiles

Exceptions to the above-given argument are expected in cases of very low frequency, large amplitude modes, and in cases where there is a resonance, or near resonance, of vi-

TABLE II. Vibrational lifetimes calculated from apparent homogeneous linewidths in He nanodroplets (except Ar–HF, measured directly). The entry under the header ''Note'' refers to the cause of vibrational relaxation; ''Tentative'' indicates that vibrational relaxation is *assumed* as the dominant cause of broadening.

Molecule	Mode	Lifetime (ns)	Note	Reference
HCOOH	ν_1 (a)	0.12	Fermi resonance	91
HCOOH	ν_1 (b)	0.09	Fermi resonance	91
HCOOH	ν_1 (c)	0.05	Fermi resonance	91
d_1–HCOOH	ν_1	0.15	Fermi resonance	91
$H^{12}C^{12}CH$	ν_3	0.12	Fermi resonance	49
$H^{13}C^{13}CH$	ν_3	≈ 1	Fermi resonance	49
$(HCN)_2$	ν_1	>0.64		66
$(HCN)_2$	ν_2	0.15	Dissociation	66
$(HF)_2$	ν_2	>0.53	Dissociation	66
$(HF)_2$	$\nu_2+\nu_5$	7×10^{-3}	Tentative	66
$(HF)_2$	$\nu_1+\nu_4$	3×10^{-3}	Tentative	66
Ar–HF	ν_1	1.5×10^{6}		84
SF_6	ν_3	0.56	Tentative	29
CH_3CCH	$2\nu_1$	0.16–1.5	Tentative	69

brational levels in a molecule and the optical excitation accesses an upper component of the resonance polyad. This can be compared to the behavior in the gas phase, where it is well established that anharmonic resonances allow for rapid (i.e., approaching the speed expected for rotational relaxation) V–V collisional relaxation inside the set of coupled levels.

A related phenomenon is the case of molecules which in the gas phase have a density of states slightly below that required for IVR via high-order relaxation, such as propyne in the $2\nu_1$ mode. In helium, the effective density of states is raised, as the helium can be excited with one or more low energy quanta, thus accommodating small energy mismatches. Molecules with a sufficiently high density of states to undergo statistical IVR in the gas phase, such as $(CH_3)_3SiCCH$,[69] are at most weakly affected by the helium.

An interesting case occurs when, in the gas phase, excitation would cause the molecule to dissociate. While the helium forms a ''cage'' which may prevents dissociation, it would still accommodate some of the excitation energy. As in the above-mentioned case, one might still be left with an excited species, but as for determining the lifetime, the initially excited state would appear to have relaxed. So far this scenario has only been observed for van der Waals complexes, and the lifetimes are only moderately decreased relative to their gas phase value. All the values measured to date are reported in Table II.

All the experimental evidence currently available indicates that the line profiles are determined by rotational relaxation only when the energy of one rotational quantum is sufficient to excite bulk modes of the droplet.[149] As the energy must then be near or above the roton minimum of 8.58 K,[102] only small molecules, with large rotational constants, display this kind of behavior. The observed lines are Lorentzian, with widths around 1 cm^{-1}, reflecting relaxation times in the 1–10 ps range (see Table III).

TABLE III. Rotational lifetimes measured in He nanodroplets. The entry in the column ''Note'' refers to the droplet modes responsible for rotational relaxation.

Molecule	Levels or band	Lifetime (ns)	Note	Reference
HCN/DCN	$J=0$	~ 10	Surface?	77
HCCCN	$J=3,4$	2–20	Surface?	76
HCCCN	$J=2,4$	10–100	Surface?	18
HF	$\nu=1,\ J=1$	12×10^{-3}	Bulk	67
$(HF)_2$	$\nu_1,\ K=1$	2.7×10^{-3}	Bulk	66

2. Indirect measurements: Saturation, double resonance

For large molecules, the dissipation channel into bulk helium modes is closed for thermally populated rotational states, and relaxation must occur either by R–T (rotation–translation) transfer (for which Franck–Condon factors are unfavorable)[95] or by coupling to the softer surface modes of the droplet. Because long-range forces confine the molecule to spend most of its time away from the surface, the latter coupling is weak, and relaxation times are correspondingly extended into the nanosecond range (see Table III). In fact, the coupling to the surface modes has been estimated to be so weak[95] that it is an outstanding question how the molecules can come to equilibrium with such a grainy heat bath. Lines are then inhomogeneously broadened, but homogeneous widths can still be estimated from saturation and double resonance measurements.

The first such measurement, the MW–MW experiment on HCCCN,[76] faced a set of apparently contradictory findings: the single resonance saturation data demonstrated that the strength of rotational lines was proportional to the square root of the applied power over a wide range, the classic signature of saturation of a line dominated by inhomogeneous broadening.[79] As the only previously considered source of inhomogeneous broadening was the spread of droplet sizes, a standard analysis based on the assumption of ''static'' broadening predicted that double resonance measurements would directly reveal the homogeneous component of the line via hole burning with the pump field, i.e., a Bennet hole and hill in the absorption of the probe,[79] with a width of no more than 150 MHz. It was instead found that the linewidths of the transitions affected by the pump beam were comparable to those measured in single resonance (1 GHz). The contradiction was solved by ascribing inhomogeneous broadening to the spectral diffusion of the dopant over a set of quantum states (most likely different translational states within the droplet; see Sec. III B). Initially it was assumed that such diffusion occurred on a time scale faster than rotational population relaxation. Upon further analysis, it was realized that this would have corresponded to a much higher saturation power than was actually observed, and it was proposed that the two phenomena are occurring on the same time scale (tens of ns).[18] Despite the use of a simplified model, and the tentative value of the parameters obtained from it, the conclusion that spectral diffusion and rotational relaxation both occur because of the motion of the dopant inside the droplet appears to be reasonable; indeed the time scale for such motion is in the ns range.

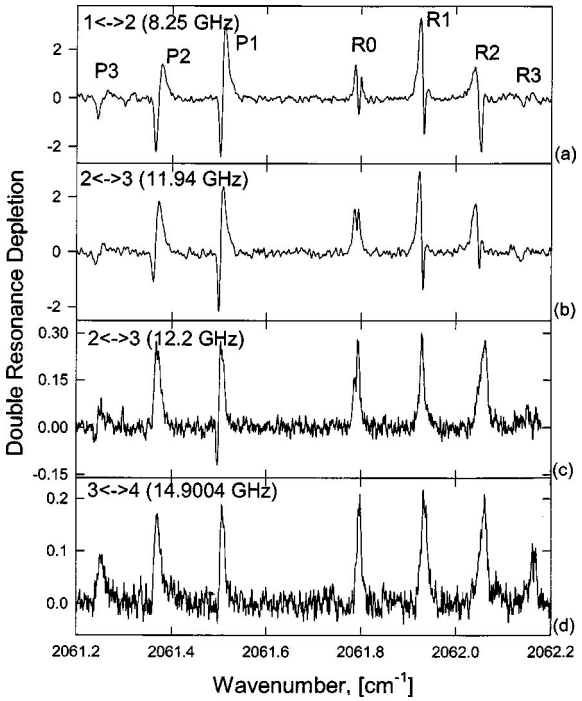

FIG. 6. Double resonance spectra of OCS in He droplets. The levels coupled by the MW ''pump'' and the frequency of the transition are indicated in the upper left-hand corner of each panel. In contrast to what is commonly observed in gas phase experiments, note how *all* the levels are affected by the MW ''pump,'' and how the total signal does not sum to zero. From Ref. 80.

MW–IR experiments performed on HCCCN[18] and OCS[80] confirmed the picture presented above: double resonance lines span the whole inhomogeneous width. A reproducible substructure of five peaks, about 50 MHz wide is observed for the $J=2\rightarrow3$ rotational transition of OCS, suggestive of a $2J+1$ splitting, but no pattern is resolved for other lines, thus making a definite assignment not possible. The main finding, common to both experiments, and therefore probably of general nature, is that the populations of *all* the rotational levels are altered by the MW ''pump'' (Fig. 6).

In gas phase DR experiments, such as the classic IR–MW studies by Oka,[103] one can often observe collisionally induced four level DR signals, but they are typically considerably weaker than the collisionless features. In helium, the relaxation induced signals have been found to be even stronger than the ''direct'' signals in some cases. There also was a strong dependence of the DR signals on the source conditions, which suggests that the relaxation dynamics are strongly dependent upon droplet size, which affects the density of states of the thermal bath that the molecule is coupled to. For HCCCN, the DR spectra dramatically simplify for the largest droplets, which has suggested rotational relaxation is in the ''strong collision'' limit for these droplets, i.e., that the relative populations produced by relaxation are independent of the initially populated state.

A curious feature observed for both HCCCN and OCS is that there appears to be a lack of conservation of population in the DR experiment. For DR signals that arise from population transfer, the integral of the DR signal over the rotation structure of the IR band should be zero since the integral cross section for IR absorption is independent of the lower state. This apparent lack of population conservation must reflect some ''artifact'' in the experiments, but the ones considered do not appear consistent with the observations; in particular, the sign of the total signal is opposite for the two molecules. This effect is currently unexplained and may ultimately reveal some interesting novel dynamics for these systems.

D. Molecular rotations

1. Changes in rotational constants: How is the helium moving?

An important aspect of the rotational structure of solvated molecules is that in most cases the effective rotational constants are substantially reduced from their gas phase values. For molecules with rotational constants much larger than 1 cm^{-1} the change on going into helium is small, while for heavier molecules the rotational constant is typically reduced by a factor of 3–4 upon helium solvation. Clearly, when the molecules rotate in helium, at least some of the helium must also move, creating kinetic energy and contributing to the effective moment of inertia of the molecular rotation. Several models have been put forward to describe the nature of the helium motion.

The first model that was proposed[54,90] assumed that a specific number of helium atoms were rotating rigidly with the molecule, directly contributing their moment of inertia to that of the molecule. This model appeared to work for both SF_6 and OCS, in that chemically reasonable positions and numbers of rigidly attached helium atoms were consistent with the experimentally observed changes in moment of inertia (ΔI). For OCS, the authors called this the ''donut model'' since it assumes that a ring of six He atoms is localized in the potential minimum locus around the OCS molecule. This very simple model has two problems. First, when one tries to extend it to lighter molecules such as NH_3 or HCN, even a single rigidly attached He atom would increase the moment of inertia by nearly an order of magnitude more than what is observed experimentally. Second, more recent results for the OCS–H_2 complex[55] in helium are clearly inconsistent with the ''donut model'' for OCS. In this work, it was found by isotopic substitution that a single H_2, HD, or D_2 molecule will replace one of the helium atoms in the ''donut.'' Yet, extrapolation to zero mass of the isotopomer gives a moment of inertia of the ''donut with a bit taken out'' considerably larger than for the OCS in a pure helium droplet, i.e., with a complete ''donut.''

A more sophisticated ''two fluid'' model for the motion of the helium was introduced by Grebenev *et al.*[15] They proposed that the density of helium around the molecule be partitioned into spatially dependent normal and superfluid fractions, with the normal fraction having large values only in the first solvation layer. In analogy with the classical Andronikashvili experiment (where the normal fluid fraction of bulk helium follows the rotation of a stack of plates, contributing to their effective moment of inertia),[104] these authors propose that the normal fluid fraction rotates rigidly with the molecule, contributing the classical moment of inertia of the normal fluid mass density. This model was incomplete, however, in that the authors provided no definition of the spa-

tially dependent normal fluid density that appears in the expression for the increase in moment of inertia.

Kwon and Whaley proposed an *ansatz* for a local superfluid density,[105] based upon an extension of Ceperley's global estimator for the bulk superfluid density from path integral Monte Carlo (PIMC) calculations.[30] They took the difference in total density and superfluid density to be a nonsuperfluid density that rotates rigidly with the molecule, assuming the molecule–He interaction is sufficiently anisotropic. The term ''nonsuperfluid density'' is used instead of ''normal fluid density'' because this density is not related to the normal fluid density produced by a ''gas'' of elementary excitations, as in bulk helium experiments such as the Andronikashvili experiment. The inertial response of the helium to rotation is a second rank tensor, involving both the axis of rotation and the direction of the response, which is measured in PIMC by a projected area of closed Feynman paths.[30] The Kwon–Whaley estimator produces a scalar superfluid density, and thus has the wrong symmetry to describe the helium inertial response.[106,107] This two fluid model has, however, made predictions in excellent agreement with experiment for the cases of SF_6 and OCS in helium. Draeger and Ceperley have proposed a new local superfluid density estimator that has the correct tensor properties and gives, when spatially averaged, the correct value for the global superfluid fraction.[107]

An alternative, quantum hydrodynamic model has also been developed for the helium contribution to the moment of inertia of molecules in helium. It is well known that linear motion of a rigid body through an ideal (aviscous and irrotational flow) fluid generates motion in the fluid that contributes to the effective mass for translation. For example, for a sphere, the effective mass increase is exactly one half of the mass of the displaced liquid.[108] Similarly, rotation of an ellipsoid generates helium kinetic energy proportional to the square of the angular velocity, thus contributing to the effective moment of inertia. The possible inclusion of such a ''superfluid hydrodynamic'' term was already recognized by Grebenev *et al.*[15] However, attempts to estimate this term, using classical expressions for the moment of inertia of an ellipsoid in a uniform fluid of the density of bulk helium, gave results which were only a small fraction of the experimental values.[15,95] On the other hand, as the density around a molecule is highly nonuniform, Callegari *et al.*[109] have developed a quantum hydrodynamic model that properly takes into account the anisotropy of the density, and have obtained moments of inertia in good agreement with experiments for a number of molecules.

If one adiabatically separates the helium motion from the rotation of the molecule, then one expects the helium density in the rotating frame of the molecule to be constant and equal to that around a static molecule.[109,110] This is called the adiabatic following approximation and, on physical grounds, should be accurate when the minimum rotational spacing, $2B$, is well below the energy of the roton, which characterizes the helium density excitation energy on the atomic level (in the two fluid model, Kwon *et al.* have introduced a distinct definition of adiabatic following).[105,111] If one further assumes that the fluid velocity field generated by this time-dependent helium density in the laboratory frame is irrotational (which Kelvin proved to be the lowest kinetic energy solution),[112] then one obtains from the equation of continuity a second-order differential equation for the velocity potential (the instantaneous laboratory frame velocity is the negative gradient of this velocity potential). The helium contribution to the moment of inertia is then calculated directly as an integral over the velocity potential. In applying this method to molecules of cylindrical symmetry, the helium density was calculated using a density functional (DF) approach[113,114] which, instead of searching for the ground state of the helium many-body problem, finds the solution of a one-particle problem with a nonlocal self interaction, whose density distribution, if the correct functional were used, would exactly match the density of the many-body wave function. It takes orders of magnitude less computational effort to solve for the helium density by DF methods than by Monte Carlo methods, and the results have been found to be in good agreement for cases where the molecule-helium interaction potentials are not too deep.[115]

An alternative derivation[116] of the quantum hydrodynamic approach is to write the many-body helium wave function in a rotating ''external'' molecular potential as that of the instantaneous static ground state wave function times a single particle phase function. Variational optimization of the energy with respect to this phase function gives the same hydrodynamic equation as for an ideal classical fluid with the adiabatic following approximation. Within a Hartree approximation for the helium wave function (which DF theory implicitly invokes), the hydrodynamic treatment gives the exact wave function correction to first order in angular velocity and thus the energy to second order. Time reversal symmetry implies that changes in the helium density can only depend on even powers of the angular velocity, and will therefore contribute only to the centrifugal distortion constant, not to the rotational constant. It has been known since the dawn of quantum mechanics[117,118] that quantum mechanics can be formulated *exactly* as a hydrodynamic problem in configuration space. The one-body approximate hydrodynamic approach used for these calculations is equivalent to many calculations that have been done in bulk helium, including the structure of the core of a vortex,[119] which has a helium density structure on a length scale smaller than that induced by the solvation of most molecules.

The quantum hydrodynamic model has been applied to a number of molecules, including HCN, HCCH, $HCCCH_3$, OCS, HCCCN, and HCN dimer.[109] For the last four, for which the adiabatic following approximation is expected to hold, the predicted increase in moment of inertia was between 103% and 130% of the observed values, as good as could be expected given the uncertainties in the helium solvation densities. For HCN and HCCH, which have small moments inertia, the hydrodynamic calculations significantly overestimate the observed increase, which is taken as evidence of the breakdown of the adiabatic following (see below). Kwon *et al.*[111] have reported that the hydrodynamic model predicts for SF_6 an increase in the moment of inertia of only 6(9)% of the experimentally observed value when their calculated superfluid (total) helium solvation density

was used. Similar hydrodynamic calculations have been done by Lehmann and Callegari[120] using the lowest four tensor components in the expansion of the helium density in octahedral harmonics. These authors find that when the total helium density is used, the hydrodynamic contribution to the moment of inertia was 55% of the observed value, and this value is likely to increase if the full anisotropy of the helium density is included. The reason for the discrepancy in the two reported values[111,120] for the hydrodynamic prediction for SF_6 has not yet been resolved.

Despite their apparent differences, the ''two fluid'' and the hydrodynamic approaches to the superfluid helium rotation problem are related. They are both based on a linear response of the helium, and thus not applicable when the adiabatic separation of molecular rotation and helium motion breaks down. Furthermore, the ''nonsuperfluid'' helium accounts for much of the angular anisotropy of the helium density, which is the source term in the quantum hydrodynamic treatment.

Clearly, it would be desirable to develop a theoretical method to directly calculate the rotational constant of molecules in superfluid helium without making the dynamical approximations of either the ''two fluid'' or quantum hydrodynamic approaches. It would also be desirable to directly calculate relaxation rates for excited rotational states as well as their energies. Unfortunately, this is still largely an unsolved problem. Blume *et al.*[121] have used an excitation energy estimator based upon the rate of decay of an approximate excited state wave function under imaginary time propagation (POITSE method). Unfortunately, only studies of very small clusters have been published to date with this method, and thus its relevance to rotational dynamics in helium nanodroplets is not established. Further, the initial state had the same rotor based nodal surfaces and thus the accuracy of this method may also depend upon an approximate adiabatic separation of the rotational motion from that of the helium. If this approximation breaks down, the initial state will contain sizable contributions from several excited states and the imaginary time propagation will contain sizable contributions from many exponential decays. Lee *et al.*[110] have calculated the rotational constant of SF_6-He_N $(N=1-20)$ by a fixed-node diffusion Monte Carlo method. In these calculations, the helium and the molecule moved in the same coordinate system, a condition that is particularly easy for a spherical top molecule, but harder in general. Calculations for the rotational spacings of SF_6 were in quantitative agreement with experiment for $N \geqslant 8$, as in the simple model proposed earlier by Hartmann *et al.*[54] The fixed node approximation used, based upon the nodes of the rotational wave function of the isolated molecule, was justified by precisely the same type of adiabatic separation of time scales that is used for adiabatic following in the quantum hydrodynamic approach.[110] Recent work on a model system[122] has found that the hydrodynamic and this molecular rotor based fixed node approximation are closely related, and break down at about the same point when the rotational constant of the molecule is increased. To date, the diffusion Monte Carlo calculations have been published only for SF_6, so the accuracy of the method in general is hard to judge, though it is likely the most accurate of the presently available methods.

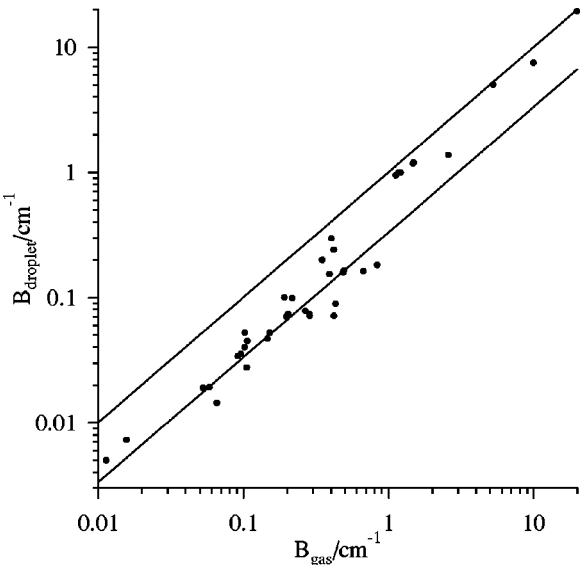

FIG. 7. Plot of the rotational constants (gas phase vs helium droplet) reported in Table I. The two lines are the functions $y=x$ and $y=x/3$, respectively. Note the different trend above and below $B_{gas}=1\ cm^{-1}$, indicative of a threshold for adiabatic following.

2. Breakdown of helium adiabatic following

As mentioned in the beginning of Sec. III D 1, ''light'' molecules with large gas phase B values appear to have little helium contributions to their moments of inertia. It is certainly the case that these molecules, by their nature, have relatively weakly anisotropic interaction potentials with the helium, and thus a small increased moment of inertia is expected. However, because they also have very small molecular moments of inertia, even a small helium contribution would be expected to lead to a substantial fractional change in the value of B. This suggests that something else is going on. The models discussed previously invoke ''adiabatic following'' of the helium with the molecular rotation, though the precise meaning of that phrase is different for the quantum hydrodynamic and the ''two fluid'' models. It is expected that this adiabatic separation of the time scales of molecular rotation and helium motion will break down when the rotational spacing becomes comparable to the energy required to create a helium excitation with a wavelength on the order of the solvation structure around the molecule, and this will be similar to the energy of the helium roton, 8.58 K.[102] This suggests a rotational constant of ≈ 4.3 K as the point where substantial breakdown of the adiabatic following would be expected (see Fig. 7). Lee *et al.*[110] studied adiabatic following breakdown theoretically by changing the rotational constant of SF_6 in their fixed node DMC calculations of small SF_6-He_N clusters. They found that the angular anisotropy of the helium in the molecular frame and the helium contribution to the effective moment of inertia both decreased substantially when the SF_6 rotational constant used in the calculation was increased by a factor of ten, from $0.1 \rightarrow 1\ cm^{-1}$. HCN ($B=2.13$ K)[123] is one of the few molecules that have been studied which is near this threshold.

The breakdown of adiabatic following for HCN has been established experimentally, by observation of the change in the helium contribution to the effective moment of inertia by isotopic substitution of HCN to DCN. Compared to DCN, it was found that the somewhat lighter and thus 23% faster HCN produced a 9% decrease in the helium contribution to the moment of inertia.[77] It would be highly desirable to study other molecular systems in this important intermediate region.

Density-functional computations can reproduce the breakdown of adiabatic following to some degree by explicitly moving the density computation from the inertial lab frame to the frame rotating with the dopant molecule. In terms of the helium and total angular momentum operators $\boldsymbol{L}$ and $\boldsymbol{J}$, respectively, the rotating-frame rotational energy of the dopant molecule is $B(\boldsymbol{J}-\boldsymbol{L})^2=BJ^2+BL^2-2B\boldsymbol{J}\cdot\boldsymbol{L}$.[124] In the rotational ground state, $\langle J^2\rangle=0$, and $\langle \boldsymbol{L}\rangle=0$ because of time reversal symmetry. Therefore, the only change in going to the rotating frame is the appearance of a term BL^2 in the helium density functional. For large values of B, this term increases the angular smoothness of the ground state helium density, which decreases the helium moment of inertia in the hydrodynamic theory; this provides a scale to gauge the breakdown of adiabatic following. Work is in progress in our group to quantitatively assess this approach.

3. Giant centrifugal distortion constants

Another interesting generic feature that has been observed in rotational spectra in helium droplets is a dramatic increase in the centrifugal distortion constants required to fit the spectra. Values of $D/B\sim10^{-4}$ have been observed for heavy molecules, three to four orders of magnitude larger than for the same molecules in the gas phase. It has been suggested that these large distortion constants reflect weakly bound helium atoms that are easily displaced by the centrifugal potential, but a careful attempt to estimate this effect, for OCS, gave a predicted D value 50 times smaller than is observed experimentally.[90] If one uses the standard scaling $D\sim4B^3/\omega^2$, one must invoke an effective vibrational wave number on the order of $1\,\mathrm{cm}^{-1}$ in order to reproduce the observed D values, much smaller than what is physically reasonable considering the force constants of the helium-molecule potentials. Given the above-mentioned discussion of the breakdown of adiabatic following with increasing rotation rate, one can argue that the effective D value should be negative, the opposite sign from what has been observed! This is because we would expect the effective B value to increase, going toward the gas phase value, as the rotational velocity increases, making it harder for the helium to follow.

At present, there is only one calculation that has reproduced the correct size of the distortion constant: a toy model[122] of a rigid, planar ring of N He atoms interacting with a rotating molecule. What this calculation clearly demonstrated is that opposite behaviors are found depending on how the rotational velocity is increased: by decreasing the moment of inertia of the molecular rotor or by spinning up a fixed rotor to higher J values. In the former case, the helium follows more poorly, consistent with the previous discussion. In the latter case, the He anisotropy and following increase until a resonance between the molecular and helium ring rotations occurs. These results are consistent with general conclusions previously drawn by Leggett in his analysis of the ''rotating bucket'' experiment for bulk liquid helium.[125]

4. Vibrational dependence of rotational constants

As in the gas phase, the effective rotational constants change upon vibrational excitation. The size of the observed vibration-rotation coupling is much larger in helium than that expected based upon the gas phase change in B. For example, for HCCCN the total increase in moment of inertia upon vibrational excitation changes from 0.35 u Å^2 in the gas phase to 9.2 u Å^2 in helium, and for CH_3CCH it changes from 0.32 u Å^2 to 8.5 u Å^2.[69] This suggests that most of the effect is due to a change in the helium contribution to the effective moment of inertia. As expected, the excited vibrational states have increased helium contributions, which suggests increased density and/or anisotropy around the vibrationally excited state. As pointed out previously, the absence of phonon wings to the spectra indicate that these changes must be small. There has yet to be published a quantitative attempt to calculate this change in solvation structure, which requires knowledge of the vibrational dependence of the molecule–He interaction potential, which is not yet generally available. Recently, there has been important progress made in the calculation of the intermolecular-mode dependence of the interaction potentials,[126] which would allow such an estimate to be made.

E. Shift in band origins

An extremely attractive feature of rovibrational spectroscopy in helium is that solvent shifts of the vibrational origins are generally quite small, typically less than 0.1%. This can be contrasted with spectroscopy in the traditional matrix environments of Ne or Ar, for which the shifts are usually much larger. As an example, for HF the matrix shifts are 0.067%, 0.24%, and 1.1%, respectively.[127] The small shifts in helium are due in large part to its low density and polarizability (even when compared to other rare gases). However, existing evidence suggests that there is often a fortuitous cancellation of effects leading to smaller shifts than one could otherwise expect.

In considering the shift in band origin, one must distinguish between the *vertical* and *adiabatic* excitation energies. The former refers to a transition within a frozen helium solvation density, while the latter considers the optimized helium solvation density in each vibrational state. As discussed previously, the observed vibrational dependence of the effective rotational constants is largely a result of such a change in helium solvation. The peak of the zero phonon line should provide an experimental estimate for the adiabatic excitation energy while the vertical excitation will be at the ''center of gravity'' of the entire transition, including the phonon wing. The difference between vertical and adiabatic excitation energies reflects the helium reorganizational energy during vibrational excitation. Given the lack of observed ''phonon side bands'' in vibrational spectra, one can anticipate that this reorganizational energy is small, but not necessarily small compared to the typically observed helium induced vibra-

tional frequency shift. If a ≈ 10 cm^{-1} wide phonon wing contains 50% of the integrated intensity of a transition, it would cause a ≈ 5 cm^{-1} shift between the adiabatic and vertical excitation wave number, but this phonon wing would have a peak absorption strength less than 1% of that of the zero phonon line (assuming a linewidth of 1–3 GHz), and thus could be easily lost in any low frequency noise in the spectrum. The vertical excitation energy, in contrast, is much easier to estimate theoretically, since it does not require computation of the change in helium–helium interactions. As an example, Blume *et al.*[57] have calculated the vertical excitation wave number of HF in helium by averaging the potential difference for He interacting with $v=0$ and 1 states of HF over the ground state wave function of the system.

The change in the helium–molecule interaction potential upon vibrational excitation reflects several different physical components. Based upon the natural separation in time scales between intramolecular and helium solvation motions, an adiabatic separation is appropriate and one can consider a vibrationally averaged molecule–helium interaction potential for each vibrational state.[126] If we consider excitation of a normal mode k in a molecule with dimensionless normal coordinates q_i, then in the harmonic approximation the He–molecule potential in the excited state of the normal vibration ν_k can be written as

$$V_{\text{eff}} = V_g + \sum_s \left(\frac{\partial V}{\partial q_s}\right)\langle q_s\rangle + \frac{1}{2}\left(\frac{\partial^2 V}{\partial q_k^2}\right)\langle q_k^2\rangle,$$

where V is the full interaction potential, including intramolecular coordinates, and the derivatives are evaluated at the equilibrium structure of the isolated molecule. The sum is restricted to totally symmetric vibrational modes, and $\langle q_s\rangle$ is proportional to the cubic anharmonic coupling ϕ_{skk} between the excited mode k and the symmetric mode s. Given the small changes in vibrational wave number upon solvation by helium, the harmonic approximation is expected to be adequate for rigid molecules.

The long-range interaction between He and the molecular dopant is dominated by the isotropic and $P_2(\cos\theta)R^{-6}$ terms. One contribution to the vibrational dependence of this term is the polarization stabilization of the dipole induced by vibrational motion, even in nonpolar molecules such as SF_6.[128] This term leads to a shift proportional to the IR strength of the vibrational mode. Integrating this term over an estimate for the helium solvation density gave a shift for SF_6 (Ref. 129) of about one half the observed value of -1.6 cm^{-1} (Refs, 14 and 54) (such an estimate is for the vertical, not adiabatic shift). A sizable fraction of the shift comes from the first solvation shell, for which the use of the long-range R^{-6} terms is not expected to be complete, though there may be a significant cancellation of errors between the neglect of higher order terms and damping of the dispersion series.[130] For molecules with a permanent dipole moment, one also needs to consider the changes in the vibrationally averaged dipole moment. While these changes are usually smaller than the transition moments, at least for reasonably strong IR transitions, one gets an ''interference'' with the permanent dipole moment (since the induction energy depends on $\langle\mu^2\rangle$), which can magnify the effects of a small absolute change in the dipole moment upon vibrational excitation. For excitation of the overtone of the C–H stretching mode in HCN,[69] the transition dipole and change in vibrationally averaged dipole moment lead to estimated shifts of 0.14 and 1.67 cm^{-1}, respectively. The long-range interaction between He and molecular dopants is typically dominated by dispersion interactions, not the induction terms. One can estimate the change in the induction terms from changes in the polarizability of the molecule upon vibrational excitation. For HCN, this gives an estimate of 5 cm^{-1} for the shift, substantially larger than the observed value.

All of the terms discussed so far are long range and lead to redshifts. They certainly are expected to dominate the droplet size dependence of the shift. Putting the solute in the center of the droplet and integrating the missing (compared to the bulk) interaction, one finds that the shift from bulk or infinite droplet size limit will be dominated by the R^{-6} terms and will scale as N^{-1}, where N is the number of helium atoms in the droplet.[32] Thus, a redshift toward the limiting bulk value is expected for large droplets, independent of whether the overall shift is red or blue. If one assumes that the droplet size distribution follows a log-normal distribution, then the inhomogeneous distribution of droplet sizes will also contribute a log-normal distribution of shifts away from the bulk value. This allows the N dependence of the width and shift for smaller droplets (where the inhomogeneous cluster size distribution contributes most to the spectral shape) to be used to estimate the inhomogeneous size dispersion contribution to the line shape of larger droplets.

Counteracting the above-discussed increases in long-range He attraction upon vibrational excitation (and higher order multipole contributions that have not yet been estimated) is an expected blueshift from the ''crowding'' interaction. Such an effect is due to the fact that the potential for a molecular oscillator will be in part stiffened due to the interaction with the first solvent shell, where repulsive forces are important. In a highly simplified harmonic picture of a linear X–H–He unit, the X–H stretch normal mode force constant will be increased by the H–He force constant. This leads to a blueshift of the vibrational frequencies that should be most important for vibrational motion dominated by exposed atoms and/or involving low frequency, large amplitude motions. Examples of the latter include the torsional mode of glyoxal[97] and the butterfly mode of pentacene,[78] both in the first excited electronic states. At fixed helium solvation structure, one would expect that the blue shift of a chemically unique vibrational motion, such as the C–H stretching mode of terminal acetylene compounds, would be approximately conserved. However, helium density functional theory calculations made by our group have shown that helium solvation density around this terminal C–H bond is a strong function of the rest of the molecule, which thus far has prevented the development of a quantitatively predictive theory of the expected blueshift.

The spectrum of HCN dimer provides some evidence for the importance of the blue shift induced by the local structure. For the hydrogen bound C–H stretch, Nauta and Miller[88] have observed a larger gas-to-helium-droplet red-

shift compared to the same quantity for the HCN monomer. They interpreted this as arising from an increasingly linear and thus strengthened hydrogen bond when HCN dimer is solvated in helium. However, this effect can also be interpreted as arising from a substantial reduction of the helium induced blueshift upon intermolecular complex formation since the hydrogen bonded H atom no longer pushes directly on the helium solvent.

At present, we lack an effective theory to use the observed solvent induced shifts to learn about the solvation structure around the chromophore molecule or to reliably predict the observed shifts, even their sign, relative to the gas phase. However, since the observed shifts appear to be small, we can safely neglect this complication in most cases, in particular when using the predictions of quantum chemistry to help assign novel spectra observed in liquid helium.

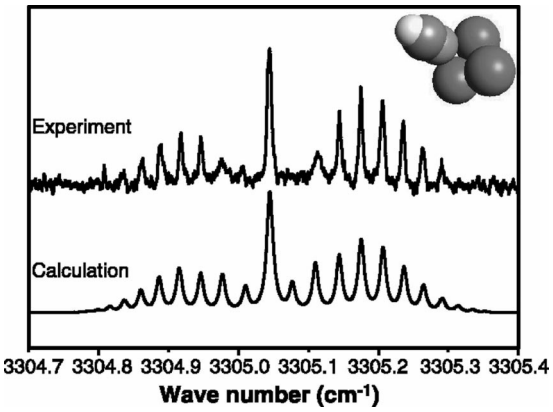

FIG. 8. Rotationally resolved spectrum of the van der Waals complex Mg_3–HCN. The structural information extracted from this spectrum allows one to deduce a contraction of the HCN–metal-cluster bond, when going from Mg_2 to Mg_3. This in turn indicates the presence of strong nonadditivity effects. From Ref. 68.

IV. SPECIAL TOPICS

A. Synthesis of nonequilibrium structures

A very promising application of HENDI spectroscopy which has been recently and dramatically demonstrated by Nauta and Miller[50,51,65] relates to the possibility of using the very cold droplet environment to synthesize highly nonequilibrium species that could not be prepared in any other known way. In analogy to the preparation of van der Waals clusters of spin polarized alkali atoms demonstrated in Princeton in 1996 (see the following review by Stienkemeier and Vilesov[131] and Refs. 132–134), the essential ingredient in these syntheses is, in addition to the low temperature of the droplets, the rapid cooling action that the superfluid helium exerts on the molecular partners at the time of cluster formation. Consider the example of the preparation of linear chains of HCN:[50] such chains with more than three monomer units have not been observed even in the cold environment of a supersonic jet expansion, where cyclic or other nonpolar structures are instead prepared. When an HCN molecule collides with a cluster that already hosts another molecule in its interior, the long range dipole–dipole forces align the two dipoles at distances where no other force is acting between the two molecules. The rapid rotational relaxation necessary for such an alignment is probably provided during multiple collisions with the droplet surface, where coupling to ripplons is enhanced. After the two dipoles have been aligned, the molecules are drawn together by their mutual attraction; in contrast to a gas phase coagulation, however, their potential energy is not completely transformed into kinetic energy because of the steady cooling action of the ''solvent.'' Consider that a potential energy of 200 K (i.e., 2.8×10^{-21} J) would accelerate a molecule of mass 27 u to a velocity of 350 m/s, which is well above the critical velocity of 60 m/s[135] above which a foreign body will rapidly dissipate energy in superfluid helium. This dissipative cooling during complexation ensures that, contrary to what happens in the gas phase, the freshly formed complex is born cold, without the energy needed to surmount any barrier to isomerization toward the global energy minimum. It is remarkable that this process is repeated until the linear chain spans the whole cluster diameter, as the data of Nauta and Miller show. Observed spectra for CH_3OH and CH_3CN clusters,[60] for H_2O clusters,[65] and for Ar_n+HF clusters (described in their article in this issue)[136] have been interpreted as arising from the isomers which are formed with the smallest amount of nuclear rearrangement.

So far this self-assembling technique has been applied using stable molecules. Efforts are in progress in our laboratory to use CN radicals for preparing isocyanogen-like chains or, if the presence of a recombination barrier is detected, at least van der Waals clusters of CN radicals. The potential applications of this technique for the synthesis of exotic or high energy density materials are quite evident.

A different, but equally useful, nonequilibrium synthesis has been demonstrated by Nauta and Miller in an experiment[68] in which a cluster of reactive metal atoms (Mg) has been attached to an IR active molecule (HCN), and the rotational spectrum of the resulting complex has been resolved (Fig. 8). While clusters of metal atoms are bound by van der Waals or metallic forces according to their size,[137–140] they are in both cases very difficult to study because their UV spectra are made of broad lines and their IR spectra, when present, appear at rather low frequencies, where lasers are not yet available. Probing the IR spectrum of a molecule attached to the atomic cluster yields valuable information on the latter via an analysis of the rotationally resolved spectrum or via the spectral shifts of the molecule's vibrations. While the information contained in rotationally resolved spectra is at present clouded by our imperfect knowledge of the helium contributions (see Sec. III D), the type of spectrum (i.e., the symmetries of complexes) and shifts are already sources of reliable information. We anticipate that this type of experiment will provide a wealth of information on metal–ligand interactions and on the nature of bonding in chemisorbed systems.

Most large organic molecules, including those of biological relevance, have a number of isomers populated at room temperature, particularly arising from rotation about single bonds (conformers). When these molecules are cooled to low temperature, either in MI or supersonic jet spectroscopies, isomers separated by high barriers do not inter-

convert, while those separated from lower-lying minima by low barriers will cool out. Multiple isomers have been observed by HENDI spectroscopy as well. As an example, see the study of glycine by Huisken *et al.*,[59] where the same three conformers were observed in He nanodroplets and in Ne and Ar matrices. In general, however, the different cooling rates should result in different distributions of conformers in the different spectroscopies. Spectra of tryptophan and tyrosine in helium have been interpreted in terms of suppression of certain conformers in helium compared to those observed in seeded beam expansions.[141] The more rapid quenching, lower final temperatures, and shorter interaction times of HENDI suggest that the conformer distribution observed by this method should more closely resemble that of the initial ensemble. The much smaller spectral shifts in helium should make conformer assignments based upon quantum chemistry calculations significantly more reliable than for MI. The use of pendular spectroscopy in helium, which allows measurement of the permanent dipole moments and the angle between that and the vibrational transition moment, should further greatly enhance reliability of assignments.

B. Large-amplitude molecular motions in liquid helium

One of the great differences between electronic and rovibrational spectroscopy in He droplets is the extent to which helium is displaced upon excitation of the molecule. Helium displacement arises from the repulsive interaction (which can be viewed in terms of the Pauli exclusion principle) between the electron clouds of He atoms and that of the molecule. Electronic excitation results in general in an expansion of the electron cloud, with an energetic cost that is responsible for the experimentally observed blueshifts of electronic spectra of atomic and molecular species immersed in liquid He. Conversely, the volume and shape of the electron cloud are not significantly changed upon rovibrational excitation. The observed band shifts are small, mostly toward the red, and are determined by a delicate balance between the attractive and repulsive forces in the ground and excited state[69] (see Sec. III E). As a first approximation, one can say that molecular stretch vibrations, with few exceptions the only modes studied so far, are too stiff to be significantly affected by the presence of the helium.

This statement does not hold true for large-amplitude modes which are, somewhat by definition, softer [the full width at half maximum of the one-dimensional harmonic oscillator is proportional to $(m\omega)^{-1/2}$ or $(km)^{-1/4}$]. They are particularly relevant not only because they displace more helium (supposedly coupling better to He bulk modes), but also because they are usually bending modes. Tunneling barriers commonly occur for such modes, and are expected to be increased by the presence of the helium. For the above-mentioned reasons, these modes are a useful probe of the molecule–helium interaction.

The prototypical transition is the ν_2 umbrella motion of NH_3:[61] the hindrance induced by the helium causes a blueshift of 17.4 cm^{-1}, an order of magnitude larger than what is commonly observed. Within the limits imposed by the coarse resolution of the spectrum (~ 1 cm^{-1}), the excited-state inversion splitting is found to be decreased by 31%. At the time, only speculations could be made as for the cause: it was suggested that helium might increase either the tunneling barrier and/or the effective mass of the oscillator, or even change the symmetry of the inversion potential, thus suppressing tunneling overall. With the knowledge we have gained in the meantime from the study of molecular rotation, we can reasonably say that the first two are going to be important while the third is probably not. Similar observations have been made for the ν_1 and ν_2 modes of the ammonia dimer.[60] In this system the inversion tunneling is already suppressed by the partner molecule, and the presence of the helium has, if any, a smaller effect. For the same reason, the large blueshift observed for the monomer is not present here. Interchange tunneling is instead affected by the presence of the helium: the splitting is reduced from 5–10 cm^{-1} to 2 cm^{-1}.

A capital step forward is the study of the HF dimer by Nauta and Miller:[66] the use of a low power continuously tunable laser and the added diagnostics provided by Stark fields allowed a truly quantitative study of tunneling motions. The interchange tunneling splitting, like in the ammonia dimer, is observed to be decreased, by an amount that is accurately quantified (-41%). Nauta and Miller propose that this is due to an increased barrier; the barrier increase is explained with the observation that the transition state is nonpolar, and hence has less energy gain from polarization of the helium than the polar equilibrium states. While it is difficult to rule out additional contributions, such as those proposed for ammonia, this one must definitely be present, since the simple model used in Ref. 66 shows quantitative agreement with the experiment. Nauta and Miller observe that this interpretation also explains a rather unusual observation. The *A* rotational constant is *increased* (from 31.96 to 33.3 cm^{-1}) upon solvation in helium, a fact which is indicative of a more linear structure. Such a structure exhibits a larger dipole moment, and is therefore consistent with a polarization energy gain.

The experiment also measured the $\nu_2+\nu_5$ and $\nu_1+\nu_4$ bands, from which the frequencies of the soft modes involving the van der Waals bond (ν_4, intermolecular stretch, and ν_5, intermolecular bend) are reconstructed. Both are found to be increased, relative to the gas phase, by $\approx 4\%$ (~ 133 cm^{-1} up from 127.57, and ~ 185 cm^{-1} up from 178.67, respectively), which is a huge value compared to any other mode observed so far. This observation is in line with the general expectation that soft modes will be more strongly affected by the hindering presence of the helium.

C. ^{3}He and mixed ^{4}He/^{3}He droplets

At present, rotationally resolved infrared spectra in pure or mixed ^{3}He droplets have been only obtained for of SF_6 (Refs. 35 and 42) and OCS.[15,90] In mixed droplets the slightly lower zero point energy of ^{4}He atoms favors their localization around the dopant molecule.[142] Thus a small doped ^{4}He cluster within the large ^{3}He droplet is formed; clusters with a small number of ^{4}He atoms ($N_4=20-30$) produce considerably broadened spectra (ascribed to inho-

mogeneous broadening induced by the spread of N_4). Otherwise the resulting spectra are, to first approximation, the same as in pure ^{4}He, except the temperature is lower (0.15 K), being dictated by evaporation of ^{3}He. As the concentration of ^{4}He in the expanding gas mixture is increased from 0.1% to 4% the temperature rises gradually to the limit value of pure ^{4}He droplets, 0.38 K.[42]

Because of the lower number density of ^{3}He, the matrix shift of the band origin (Sec. III E) is also affected. The band origin shift of SF_6 has been used to estimate the number of ^{4}He atoms in the inner cluster;[42] small shifts within the R branch suggest that the rotational constant of SF_6 in mixed droplets with a large number of ^{4}He atoms (200–500) is $\approx$3% larger than in pure ^{4}He droplets. The effect is more evident for OCS, where the rotational constant drops by up to 10%, at $N_4=60$.[143,144]

Studies of isotopically pure ^{3}He droplets were limited to OCS which has a simpler Hamiltonian and a better resolved spectrum.[15,90] Whereas in pure ^{4}He the spectrum shows the well-resolved rotational structure expected for a linear molecule, in pure ^{3}He droplets the spectrum collapses into a broad single band, very similar to what is expected in a classical fluid. Since the binary interaction potentials of OCS with ^{3}He and ^{4}He atoms are virtually identical, the difference must be due to the different states of the droplet: superfluid for ^{4}He and normal fluid for ^{3}He. Molecules in nonsuperfluid ^{3}He are rapidly exchanging their energy and angular momentum with the medium as compared to superfluid ^{4}He.[145] Thus the ability of the dopant molecule to rotate coherently over many periods is a microscopic manifestation of superfluidity. Recently, the spectrum in pure ^{3}He has also been fitted to an unresolved rotational structure; this gives a rotational constant 1.6 times smaller than in ^{4}He.[144]

The onset of superfluidity in small ^{4}He clusters has been investigated by intentionally doping an isotopically pure ^{3}He droplet containing one OCS molecule with a controlled number (up to 100) of ^{4}He atoms.[15] The gradual appearance of a sharp rotational structure indicates that the onset of superfluidity is a smooth process, and is almost complete in a cluster of just 60 ^{4}He atoms, corresponding to approximately two solvation layers. While it is understood that preservation of rotational coherence depends on a lack of accessible excitation of the helium, in turn linked to the Bose permutation symmetry of the first solvation shell(s),[122,145] the detailed mechanism of this effect is still to be understood.

Further addition of the ^{4}He atoms does not lead to qualitative change of the spectrum. The appearance of particularly sharp lines in the P branch ($<$100 MHz) has been attributed to cancellation of rotational and vibrational contributions to inhomogeneous broadening.[143]

D. Molecule/hydrogen clusters in helium droplets

The HENDI study of van der Waals clusters containing various isotopomers of molecular hydrogen deserves special attention because of the highly quantum nature of the latter molecule. Just like the magnesium clusters discussed in Sec. IV A,[68] the arrangement and properties of hydrogen molecules are studied through their effect on the infrared spectrum of a larger molecule such as OCS.[52,55,56]

The first study of an OCS–H_2 (–HD, –D_2) van der Waals complex[55] has indicated that the hydrogen molecule lies in the ring-shaped locus of the potential minimum around OCS, with a rather large delocalization out of the average OCS–hydrogen plane. It is not clear, however, to what degree the use of Kraitchman's equations (which are used to derive the position of an isotopically substituted atom from the resulting change in the moments of inertia, assuming a rigid structure)[146] is justified given the large amplitude of the hydrogen vibration. However, the resulting OCS–H_2 structure was found to be in reasonable agreement with the predictions of recent *ab initio* calculations.[147]

The same authors have found[56] that upon addition of more *para*-hydrogen molecules to the OCS–$(pH_2)_n$ van der Waals complex in pure ^{4}He (0.38 K) and mixed ^{4}He/^{3}He (0.15 K) droplets, the rovibrational spectrum rapidly approaches that of a symmetric top, until, for $n=5$ and 6, the Q branch disappears and the symmetry of the spectrum is that of a linear molecule again, just as for a pure OCS molecule in a helium droplet. This is most probably due to the fact that the bosonic ($I=0$) pH_2 molecules form a complete ring of C_{nv} ($n=5-6$) symmetry around OCS. As discussed for helium excitations in Sec. III, azimuthal excitations of such a ring are forbidden if K is not an integer multiple of n. In the cold environment of the helium droplets, such high-K levels are not populated, and there can be no Q branch.[148,149]

In the same article, a very interesting comparison has been made with the same complex but using *ortho*-deuterium (oD_2) instead of pH_2. One would expect that the six-fold nuclear spin degeneracy of oD_2 makes the probability for building a ring of indistinguishable oD_2 molecules equal to 6^{1-n}, which amounts to 0.8% for $n=5$ and 0.1% for $n=6$. The resulting decreases in intensity of the Q branches of OCS–$(oD_2)_n$ complexes are therefore negligible. Indeed, the spectra of all OCS–$(oD_2)_n$ clusters up to $n=8$ feature a Q branch.

Most surprisingly, the same authors have found[52] that the Q branch disappears again for OCS–$(pH_2)_n$ clusters with $n=14-16$ at 0.15 K, but not at 0.38 K. For these values of n, the pH_2 molecules probably form several rings around OCS, with different numbers n_i of molecules per ring. One could imagine a situation where two rings are formed, with $n_1=6$ and $n_2=8$ pH_2 molecules, with a C_{2v} structure. Based upon the results for the OCS–H_2 monomer, a moment of inertia $I_a\approx 370$ u Å^2 can be estimated for this structure. This would imply that the lowest accessible state with rotational angular moment along the OCS axis ($K=2$) will have an excitation energy of 0.26 K, allowing significant population at 0.38 K but not at 0.15 K. The next two pH_2 molecules could then be added at both ends of the OCS on the molecular axis, preserving the C_{2v} structure, and finally resulting in a filled shell of 16 pH_2 molecules around the OCS (compare to a filled ^{4}He shell that consists of 17 molecules).[111] This picture neglects any additional reduction of the rotational constant by the helium, which is expected to be small because such a highly symmetric structure may not induce much angular anisotropy in the helium. The authors of Ref. 52 propose the radically different explanation that at the lower temperature (0.15 K), large delocalization of the pH_2

molecules leads to bosonic exchange and thus to a ''superfluid'' state of the hydrogen rings, which effectively makes the symmetry group $C_{\infty v}$ and forbids any states with $K \neq 0$. At higher temperature (0.38 K), however, delocalization is less, and thermal population of $|K|>0$ states yields a Q branch. The field of $(pH_2)_n$ clusters will need further study in order to corroborate this claim of superfluidity.

V. CONCLUSION

HENDI spectroscopy has evolved from earlier molecular beam techniques for isolated and complexed atoms and molecules and has, in a rather short time, reached the point where it can be applied to the study of a wide variety of problems. Rovibrational spectroscopy in this novel extremely cold and finite environment reveals rich spectra, often with much more detail than in other condensed phases. The field has made significant progress in developing the experimental and theoretical tools needed to extract relevant information from these spectra. However, a number of fundamental questions remain which principally relate to the nature of the interactions of the molecular motions with the highly quantum many-body dynamics of the helium. We still do not understand the mechanism by which molecules come into equilibrium with the droplets, nor do we know precisely the time scales for many of the relaxation processes that occur.

Despite the fact that much work remains to be done on these basic issues, the field is also rapidly making the transition from using molecules to study the physics of the droplets to using droplets to create and study novel chemical species. Vibrational spectroscopy has produced the bulk of the results in this direction, due to the high resolution available and the nearly additive effects from multiple perturbers. New tools, especially continuously tunable IR lasers at longer wavelengths than 3.5 μm and the development of sources of radicals for pickup by the droplets, promise to greatly expand the range of chemical physics that can be done with the smallest and coldest chemical vials yet devised.

ACKNOWLEDGMENTS

The authors would like to thank Udo Buck, David Farrelly, Martina Havenith, and Andrej Vilesov for carefully reading and commenting on this manuscript. This work was supported by grants from the National Science Foundation and the Air Force Office of Scientific Research.

[1] J. P. Toennies and A. F. Vilesov, Annu. Rev. Phys. Chem. **49**, 1 (1998).
[2] K. B. Whaley, in *Advances in Molecular Vibrations and Collision Dynamics*, edited by J. M. Bowman and Z. Bacic (JAI, Greenwich, CT, 1998), Vol. III, p. 397–451.
[3] G. M. Stewart and J. D. McDonald, J. Chem. Phys. **78**, 3907 (1983).
[4] H.-C. Chang and W. Klemperer, J. Chem. Phys. **98**, 2497 (1993).
[5] R. E. Miller, in *Atomic and Molecular Beam Methods*, edited by G. Scoles (Oxford University Press, New York, 1992), Vol. 2, Chap. 6, p. 192–212.
[6] T. E. Gough, R. E. Miller, and G. Scoles, Appl. Phys. Lett. **30**, 338 (1977).
[7] D. J. Nesbitt, Annu. Rev. Phys. Chem. **45**, 367 (1994).
[8] C. E. Klots, J. Chem. Phys. **83**, 5854 (1985).
[9] J. M. Hutson, Annu. Rev. Phys. Chem. **41**, 123 (1990).
[10] T. E. Gough, M. Mengel, P. A. Rowntree, and G. Scoles, J. Chem. Phys. **83**, 4958 (1985).
[11] T. E. Gough, D. G. Knight, and G. Scoles, Chem. Phys. Lett. **97**, 155 (1983).
[12] B. Tabbert, H. Günther, and G. zu Putlitz, J. Low Temp. Phys. **109**, 653 (1997).
[13] S. Tam *et al.*, J. Chem. Phys. **111**, 4191 (1999).
[14] S. Goyal, D. L. Schutt, and G. Scoles, Phys. Rev. Lett. **69**, 933 (1992).
[15] S. Grebenev, J. Toennies, and A. Vilesov, Science **279**, 2083 (1998).
[16] K. K. Lehmann and G. Scoles, Science **270**, 2065 (1998).
[17] J. Northby, J. Chem. Phys. **115**, 10065 (2001).
[18] C. Callegari *et al.*, J. Chem. Phys. **113**, 4636 (2000).
[19] See, e.g., Advanced Research Systems; Sumitomo Heavy Industries Ltd.; Helix Technology.
[20] H. Buchenau *et al.*, J. Chem. Phys. **92**, 6875 (1990).
[21] J. Harms, J. Toennies, and F. Dalfovo, Phys. Rev. B **58**, 3341 (1998).
[22] J. Harms, J. Toennies, M. Barranco, and M. Pi, Phys. Rev. B **63**, 4513 (2001).
[23] H. Haberland, in *Clusters of Atoms and Molecules: Theory, Experiment, and Cluster of Atoms*, edited by H. Haberland [Springer Ser. Chem. Phys., **52**, 205 (1994)], Chap. 3.
[24] R. A. Smith, T. Ditmire, and J. W. G. Tisch, Rev. Sci. Instrum. **69**, 3798 (1998).
[25] E. L. Knuth, B. Schilling, and J. P. Toennies, in *19th International Symposium on Rarefied Gas Dynamics, University of Oxford, 1994* (Oxford University Press, Oxford, 1995), Vol. 19, p. 270–276, $\langle N \rangle$ was calculated according to the scaling law given in this reference; since no explicit dependence of $\langle N \rangle$ on the scaling parameter Γ is given, the data in Fig. 1 were fitted to a line obtaining: $\ln(\langle N \rangle) = 2.44 + 2.25 \ln(\Gamma)$.
[26] J. Harms and J. P. Toennies, J. Low Temp. Phys. **113**, 501 (1998).
[27] J. Harms, J. P. Toennies, and E. L. Knuth, J. Chem. Phys. **106**, 3348 (1997).
[28] E. L. Knuth and U. Henne, J. Chem. Phys. **110**, 2664 (1999).
[29] M. Hartmann *et al.*, J. Chem. Phys. **110**, 5109 (1999).
[30] D. M. Ceperley, Rev. Mod. Phys. **67**, 279 (1995).
[31] B. M. Abraham *et al.*, Phys. Rev. A **1**, 250 (1970).
[32] J. Jortner, Z. Phys. D: At., Mol. Clusters **24**, 247 (1992).
[33] J. Gspann, in *Physics of Electronic and Atomic Collisions*, edited by S. Datz (North-Holland, Amsterdam, 1982), p. 79.
[34] D. Brink and S. Stringari, Z. Phys. D: At., Mol. Clusters **15**, 257 (1990).
[35] J. Harms *et al.*, J. Mol. Spectrosc. **185**, 204 (1997).
[36] Beam Dynamics, Inc., Eden Prairie, MN.
[37] D. L. Miller, in *Atomic and Molecular Beam Methods*, edited by G. Scoles (Oxford University Press, New York, 1988), Vol. 1, Chap. 2, pp. 17–53.
[38] P. Stephens and J. King, Phys. Rev. Lett. **51**, 1538 (1983).
[39] J. Gspann, Z. Phys. B: Condens. Matter **98**, 405 (1995).
[40] M. Farnik, U. Henne, B. Samelin, and J. Toennies, Phys. Rev. Lett. **81**, 3892 (1998).
[41] J. Harms and J. Toennies, Phys. Rev. Lett. **83**, 344 (1999).
[42] J. Harms *et al.*, J. Chem. Phys. **110**, 5124 (1999).
[43] Isotec, Inc. \$175/L for 99.95% and \$280/L for Grade 6, both at STP.
[44] W. Schöllkopf and J. Toennies, Science **266**, 1345 (1994).
[45] R. Guardiola and J. Navarro, Phys. Rev. Lett. **84**, 1144 (2000).
[46] M. Barranco, J. Navarro, and A. Poves, Phys. Rev. Lett. **78**, 4729 (1997).
[47] S. A. Chin and E. Krotscheck, Phys. Rev. B **52**, 10405 (1995), the binding energy per atom (E, in K), as a function of droplet size N, is given by: $E = -7.21 + 17.71N^{-1/3} - 5.95N^{-2/3}$.
[48] M. Lawerenz, B. Schilling, and J. P. Toennies, J. Chem. Phys. **102**, 8191 (1995).
[49] K. Nauta and R. E. Miller, J. Chem. Phys. **115**, 8384 (2001).
[50] K. Nauta and R. E. Miller, Science **283**, 1895 (1999).
[51] K. Nauta, D. T. Moore, and R. E. Miller, Faraday Discuss. **113**, 261 (1999).
[52] S. Grebenev, B. Sartakov, J. Toennies, and A. Vilesov, Science **289**, 1532 (2000).
[53] S. Goyal, D. L. Schutt, and G. Scoles, J. Phys. Chem. **97**, 2236 (1993).
[54] M. Hartmann, R. E. Miller, J. P. Toennies, and A. Vilesov, Phys. Rev. Lett. **75**, 1566 (1995).
[55] S. Grebenev, B. Sartakov, J. Toennies, and A. Vilesov, J. Chem. Phys. **114**, 617 (2001).
[56] S. Grebenev *et al.*, Faraday Discuss. **118**, 19 (2001).
[57] D. Blume, M. Lewerenz, F. Huisken, and M. Kaloudis, J. Chem. Phys. **105**, 8666 (1996).
[58] R. Fröchtenicht, M. Kaloudis, M. Koch, and F. Huisken, J. Chem. Phys. **105**, 6128 (1996).

[59] F. Huisken, O. Werhahn, A. Y. Ivanov, and S. A. Krasnokutski, J. Chem. Phys. **111**, 2978 (1999).
[60] M. Behrens *et al.*, J. Chem. Phys. **107**, 7179 (1997).
[61] M. Behrens *et al.*, J. Chem. Phys. **109**, 5914 (1998).
[62] M. Behrens *et al.*, J. Chem. Phys. **111**, 2436 (1999).
[63] M. Kunze *et al.*, Z. Phys. Chemie-Int. J. Res. Phys. Chem. Chem. Phys. **214**, 1209 (2000).
[64] K. Nauta and R. E. Miller, Phys. Rev. Lett. **82**, 4480 (1999).
[65] K. Nauta and R. E. Miller, Science **287**, 293 (2000).
[66] K. Nauta and R. E. Miller, J. Chem. Phys. **113**, 10158 (2000).
[67] K. Nauta and R. E. Miller, J. Chem. Phys. **113**, 9466 (2000).
[68] K. Nauta, D. T. Moore, P. L. Stiles, and R. E. Miller, Science **292**, 481 (2001).
[69] C. Callegari *et al.*, J. Chem. Phys. **113**, 10535 (2000).
[70] U. Even *et al.*, J. Chem. Phys. **112**, 8068 (2000).
[71] P. E. Powers, T. J. Kulp, and S. E. Bisson, Opt. Lett. **23**, 159 (1998).
[72] F. Capasso, C. Gmachl, D. L. Sivco, and A. Y. Cho, Phys. World **12**, 27 (1999).
[73] R. Colombelli *et al.*, Appl. Phys. Lett. **78**, 2620 (2001).
[74] See Ref. 23.
[75] H. Fröchtenicht, J. P. Toennies, and A. F. Vilesov, Chem. Phys. Lett. **229**, 1 (1994).
[76] I. Reinhard *et al.*, Phys. Rev. Lett. **82**, 5036 (1999).
[77] A. Conjusteau *et al.*, J. Chem. Phys. **113**, 4840 (2000).
[78] M. Hartmann, A. Lindinger, J. P. Toennies, and A. F. Vilesov, J. Phys. Chem. A **105**, 6369 (2001).
[79] W. Demtröder, *Laser Spectroscopy*, 2nd ed. (Springer, Berlin, 1996).
[80] S. Grebenev *et al.*, J. Chem. Phys. **113**, 9060 (2000).
[81] *CRC Handbook of Chemistry and Physics*, 70th ed., edited by R. C. Weast (CRC Boca Raton, FL, 1990).
[82] J. Reho *et al.*, J. Chem. Phys. **112**, 8409 (2000).
[83] C. H. Townes and A. L. Schawlow, *Microwave Spectroscopy* (Dover, New York, 1975).
[84] K. Nauta and R. E. Miller, J. Chem. Phys. **115**, 4508 (2001).
[85] H. J. Loesch and A. Remscheid, J. Chem. Phys. **93**, 4779 (1990).
[86] B. Friedrich, D. P. Pullman, and D. R. Herschbach, J. Phys. Chem. **95**, 8118 (1991).
[87] K. Nauta and R. E. Miller, in *Atomic and Molecular Beams: The State of the Art 2000*, edited by R. Campargue (Springer, Berlin, 2001), Part VI.3, pp. 775–793.
[88] K. Nauta and R. E. Miller, J. Chem. Phys. **111**, 3426 (1999).
[89] K. Nauta and R. E. Miller (personal communication).
[90] S. Grebenev *et al.*, J. Chem. Phys. **112**, 4485 (2000).
[91] F. Madeja *et al.*, J. Chem. Phys. (to be published).
[92] K. Nauta and R. E. Miller J. Chem. Phys. **115**, 10254 (2001).
[93] R. E. Miller, Fourth Workshop on Quantum Fluid Clusters, Ringberg Schloss, 2000.
[94] F. Dalfovo, R. Mayol, M. Pi, and M. Barranco, Phys. Rev. Lett. **85**, 1028 (1999).
[95] K. K. Lehmann, Mol. Phys. **97**, 645 (1999).
[96] F. Stienkemeier, J. Higgins, W. E. Ernst, and G. Scoles, Phys. Rev. Lett. **74**, 3592 (1995).
[97] M. Hartmann *et al.*, Phys. Rev. Lett. **76**, 4560 (1996).
[98] C. C. Hu, R. Petluri, and J. A. Northby, Physica B **284**, 107 (2000).
[99] J. P. Toennies and A. F. Vilesov, Chem. Phys. Lett. **235**, 596 (1995).
[100] K. K. Lehmann, Mol. Phys. **98**, 1991 (2000).
[101] E. Manousakis and V. R. Pandharipande, Phys. Rev. B **33**, 150 (1986).
[102] K. H. Andersen *et al.*, Phys. Rev. Lett. **77**, 4043 (1996).
[103] T. Oka, Adv. At. Mol. Phys. **9**, 127 (1973).
[104] E. L. Andronikashvili, J. Phys. (Moscow) **10**, 201 (1946).
[105] Y. Kwon and K. B. Whaley, Phys. Rev. Lett. **83**, 4108 (1999).
[106] D. M. Ceperley, paper presented at the IV Workshop on quantum fluid clusters, Ringberg Schloss, 2000.
[107] E. W. Draeger, Ph.D. thesis, University of Illinois at Urbana-Champaign, 2001, http://archive.ncsa.uiuc.edu/Apps/CMP/draeger/draeger_thesis.ps.gz
[108] H. Lamb, *Hydrodynamics*, 4th ed. (Cambridge University Press, Cambridge, 1916).
[109] C. Callegari *et al.*, Phys. Rev. Lett. **83**, 5058 (1999).
[110] E. Lee, D. Farrelly, and K. B. Whaley, Phys. Rev. Lett. **83**, 3812 (1999).
[111] Y. Kwon *et al.*, J. Chem. Phys. **113**, 6469 (2000).
[112] L. M. Milne-Thompson, *Theoretical Hydrodynamics*, 5th ed. (Dover, New York, 1996).
[113] J. Dupont-Roc, M. Himbert, N. Pavloff, and J. Treiner, J. Low Temp. Phys. **81**, 31 (1990).
[114] F. Dalfovo *et al.*, Phys. Rev. B **52**, 1193 (1995).
[115] F. Dalfovo, Z. Phys. D: At., Mol. Clusters **29**, 61 (1994).
[116] K. K. Lehmann (unpublished).
[117] E. Madelung, Z. Phys. **40**, 332 (1926).
[118] L. de Broglie, Compt. Rend. **183**, 447 (1926).
[119] G. Ortiz and D. M. Ceperley, Phys. Rev. Lett. **75**, 4642 (1995).
[120] K. K. Lehmann and C. Callegari (unpublished).
[121] D. Blume, M. Mladenović, M. Lewerenz, and K. B. Whaley, J. Chem. Phys. **110**, 5789 (1999).
[122] K. Lehmann, J. Chem. Phys. **114**, 4643 (2001).
[123] A. G. Maki, J. Phys. Chem. Ref. Data **3**, 221 (1974).
[124] J. M. Hutson, in *Advances in Molecular Vibrations and Collision Dynamics*, edited by J. M. Bowman (JAI, Greenwich, CT, 1991), Vol. 1A, pp. 1–45.
[125] A. J. Leggett, Phys. Fenn. **8**, 125 (1973).
[126] K. Szalewicz, Faraday Discuss. **118**, 121 (2001).
[127] F. Huisken, M. Kaloudis, and A. A. Vigasin, Chem. Phys. Lett. **269**, 235 (1997).
[128] D. Eichenauer and R. J. LeRoy, J. Chem. Phys. **88**, 2898 (1988).
[129] Y. Kwon, D. M. Ceperley, and K. B. Whaley, J. Chem. Phys. **104**, 2341 (1996).
[130] C. Douketis *et al.*, J. Chem. Phys. **76**, 3057 (1982).
[131] F. Stienkemeier and A. F. Vilesov, J. Chem. Phys. **115**, 10119 (2001).
[132] J. P. Toennies, A. F. Vilesov, and K. B. Whaley, Phys. Today **54**, 31 (2001).
[133] J. Higgins *et al.*, Science **273**, 629 (1996).
[134] J. Higgins *et al.*, J. Chem. Phys. **112**, 1 (2000).
[135] J. Wilks and D. S. Betts, *An Introduction to Liquid Helium*, 2nd ed. (Oxford University Press, New York, 1987).
[136] K. Nauta and R. E. Miller, J. Chem. Phys. **115**, 10138 (2001).
[137] R. Busani, M. Folkers, and O. Cheshnovsky, Phys. Rev. Lett. **81**, 3836 (1998).
[138] K. Bowen, unpublished results on Mg_n^- photoelectron spectroscopy, 2001.
[139] T. Diederich *et al.*, Phys. Rev. Lett. **86**, 4807 (2001).
[140] A. Kohn, F. Weigend, and R. Ahlrichs, Phys. Chem. Chem. Phys. **3**, 711 (2001).
[141] A. Lindinger, J. P. Toennies, and A. F. Vilesov, J. Chem. Phys. **110**, 1429 (1999).
[142] M. Pi, R. Mayol, and M. Barranco, Phys. Rev. Lett. **82**, 3093 (1999).
[143] S. Grebenev, Ph.D. thesis, Universität Göttingen, Göttingen, Germany, 2000.
[144] S. Grevenev *et al.*, Physica B **280**, 65 (2000).
[145] V. Babichenko and Y. Kagan, Phys. Rev. Lett. **83**, 3458 (1999).
[146] W. Gordy and R. L. Cook, *Microwave Molecular Spectra* (Wiley, New York, 1984).
[147] K. Higgins, as reported in Ref. 55, 1999.
[148] Nodal surfaces are necessary to separate regions of different angular momentum in the helium droplet, in order to preserve continuity of the wave function.
[149] Particularly compelling is the remarkable sharpness of the subbands that by selection rules do not rotationally relax, observed for HF, $(HF)_2$, and HCCH.
[150] K. Nauta and R. E. Miller, Chem. Phys. Lett. (to be published).
[151] D. T. Moore, M. Ishiguro, L. Oudejans, and R. E. Miller, J. Chem. Phys. **115**, 5137 (2001);D. T. Moore, M. Ishiguro, and R. E. Miller,J. Chem. Phys. **115**, 5144 (2001).